Table 3. Univariate and multivariate analyses of prognosis factors associated with overall and disease-free survival in patients with HCC

Variables	Univariate analysis		Multivariate analysis	
	Hazard ratio (95% confidence interval)	P	Hazard ratio (95% confidence interval)	P
(A) Univariate and multivariate analyses of prognosis factors associated with overall survival in patients with HCC				
Prevalence of tumor-infiltrating FOXP3$^+$ Tregs among CD4$^+$ T cells in HCC (high/low)	1.791 (1.163-2.760)	**0.008**	1.640 (1.023-2.628)	**0.040**
Prevalence of tumor-infiltrating CD8$^+$ T cells in total T cells in HCC (high/low)	1.055 (0.687-1.620)	0.806	1.109 (0.681-1.805)	0.678
Age* (≥63 y/<63 y)	1.003 (0.653-1.540)	0.989	0.909 (0.573-1.440)	0.684
Gender (male/female)	1.052 (0.636-1.740)	0.844	0.957 (0.554-1.655)	0.876
Viral hepatitis (presence/absence)	1.140 (0.496-2.620)	0.757	0.972 (0.332-2.842)	0.958
Nontumor liver (NCH/CH, PC, LC)	0.766 (0.369-1.592)	0.475	0.503 (0.207-1.225)	0.130
Child-Pugh score (A/B, C)	0.462 (0.222-0.962)	**0.039**	0.395 (0.171-0.913)	**0.030**
TNM stage (I, II/III, IV)	0.412 (0.256-0.663)	**<0.001**	1.079 (0.456-2.548)	0.863
Tumor size* (≥37 mm/<37 mm)	1.398 (0.909-2.149)	0.127	1.018 (0.553-1.875)	0.954
AFP* (≥27.1 ng/mL/<27.1 ng/mL)	1.673 (1.084-2.581)	**0.020**	1.454 (0.901-2.347)	0.125
Histologic grade (WD HCC/MD HCC, PD HCC)	0.637 (0.376-1.078)	0.093	0.931 (0.489-1.772)	0.828
VP (presence/absence)	2.843 (1.825-4.429)	**<0.001**	2.546 (1.323-4.900)	**0.005**
IM (presence/absence)	2.880 (1.786-4.641)	**<0.001**	2.081 (0.916-4.730)	0.080
Prevalence CD8$^+$ T cells in total T cells in nontumor liver (high/low)	0.754 (0.490-1.159)	0.198	0.688 (0.419-1.131)	0.140
Prevalence of FOXP3$^+$ Tregs among CD4$^+$ T cells in nontumor liver (high/low)	0.756 (0.491-1.165)	0.205	0.737 (0.442-1.229)	0.241
(B) Univariate and multivariate analyses of prognosis factors associated with disease-free survival in patients with HCC				
Prevalence of tumor-infiltrating FOXP3$^+$ Tregs among CD4$^+$ T cells in HCC (high/low)	1.701 (1.105-2.619)	**0.016**	1.706 (1.073-2.713)	**0.024**
Prevalence of tumor-infiltrating CD8$^+$ T cells in total T cells in HCC (high/low)	1.150 (0.750-1.765)	0.522	1.330 (0.817-2.165)	0.251
Age* (≥63 y/<63 y)	0.917 (0.597-1.407)	0.691	0.803 (0.508-1.271)	0.350
Gender (male/female)	0.992 (0.600-1.641)	0.976	0.941 (0.546-1.619)	0.825
Viral hepatitis (presence/absence)	0.931 (0.405-2.140)	0.866	0.754 (0.249-2.287)	0.619
Nontumor liver (NCH/CH, PC, LC)	0.902 (0.435-1.871)	0.782	0.537 (0.215-1.342)	0.184
Child-Pugh score (A/B, C)	0.458 (0.220-0.955)	**0.037**	0.463 (0.206-1.039)	0.062
TNM stage (I, II/III, IV)	0.357 (0.220-0.577)	**<0.001**	0.808 (0.320-2.038)	0.651
Tumor size* (≥37 mm/<37 mm)	1.455 (0.947-2.235)	0.087	1.171 (0.635-2.159)	0.614
AFP* (≥27.1 ng/mL/<27.1 ng/mL)	1.556 (1.010-2.397)	**0.045**	1.503 (0.932-2.421)	0.944
Histologic grade (WD HCC/MD HCC, PD HCC)	0.810 (0.481-1.365)	0.429	1.354 (0.722-2.538)	0.345
VP (presence/absence)	2.284 (1.476-3.535)	**<0.001**	1.692 (0.870-3.294)	0.121
IM (presence/absence)	3.512 (2.163-5.704)	**<0.001**	2.487 (1.020-6.064)	**0.045**
Prevalence CD8$^+$ T cells in total T cells in nontumor liver (high/low)	0.727 (0.473-1.118)	0.146	0.644 (0.393-1.054)	0.080
Prevalence of FOXP3$^+$ Tregs among CD4$^+$ T cells in nontumor liver (high/low)	0.800 (0.520-1.230)	0.309	0.788 (0.482-1.290)	0.344

Abbreviations: MD, moderately differentiated; PD, poorly differentiated; WD, well differentiated.
*Two groups were divided by the median.

Infiltration of Tregs shows no difference among different histologic types of tumor, but differs between primary and metastatic hepatic tumors. Although metastatic liver tumors are common, the most frequent type of tumor developing primarily in the liver is HCC, and the second major type is ICC. In order to examine whether antitumor immune response was affected by tumor histology, we compared the prevalence of Tregs and CD8$^+$ T cells between HCC and primary hepatic adenocarcinoma, ICC (n = 39). The prevalence of Tregs in the tumor stroma was comparable between HCC and ICC (Fig. 4A), whereas the prevalence of CD8$^+$ T cells in ICC was significantly lower than that in HCC (P = 0.004; Fig. 4A). The prevalence of Tregs in nontumorous liver was also comparable between patients with HCC and patients with ICC (Fig. 4B), although their prevalence was significantly higher than that in healthy liver (versus HCC, $P < 0.001$; versus ICC, $P < 0.001$). The prevalence of CD8$^+$ T cells in nontumorous liver was comparable among patients with HCC, ICC, and healthy liver. These findings suggest that the Treg response is almost the same in both histologic types of primary hepatic tumor, HCC, and ICC, whereas the CD8$^+$ T cell response is reduced to a greater degree in ICC than in HCC.

We then analyzed the prevalence of tumor-infiltrating Tregs and CD8$^+$ T cells in the liver of patients with primary HCC, its IM (n = 27), ICC (n = 39), and metastatic liver adenocarcinoma originating from colorectal cancer (n = 59), to examine whether the antitumor immune response differs between primary and metastatic tumors of the liver. The prevalence of Tregs

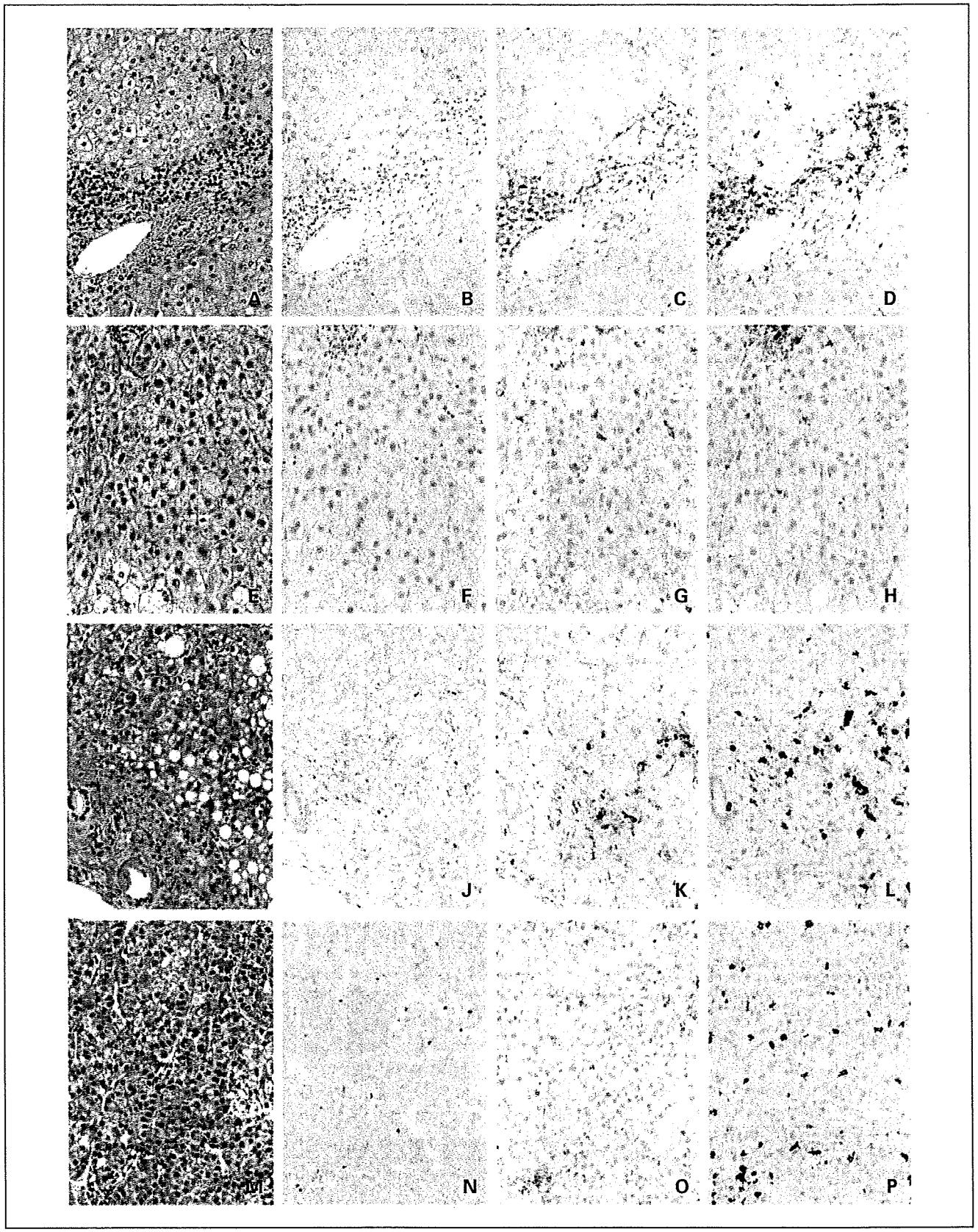

Fig. 2. Representative features of tissue-infiltrating FOXP3$^+$, CD4$^+$, or CD8$^+$ T lymphocytes. CH (*A-D*), AH (*E-H*), early HCC (*I-L*), and MD HCC (*M-P*) by HE staining (*A, E, I,* and *M*) and immunostaining for FOXP3 (*B, F, J,* and *N*), CD4 (*C, G, K,* and *O*), and CD8 (*D, H, L*, and *P*).

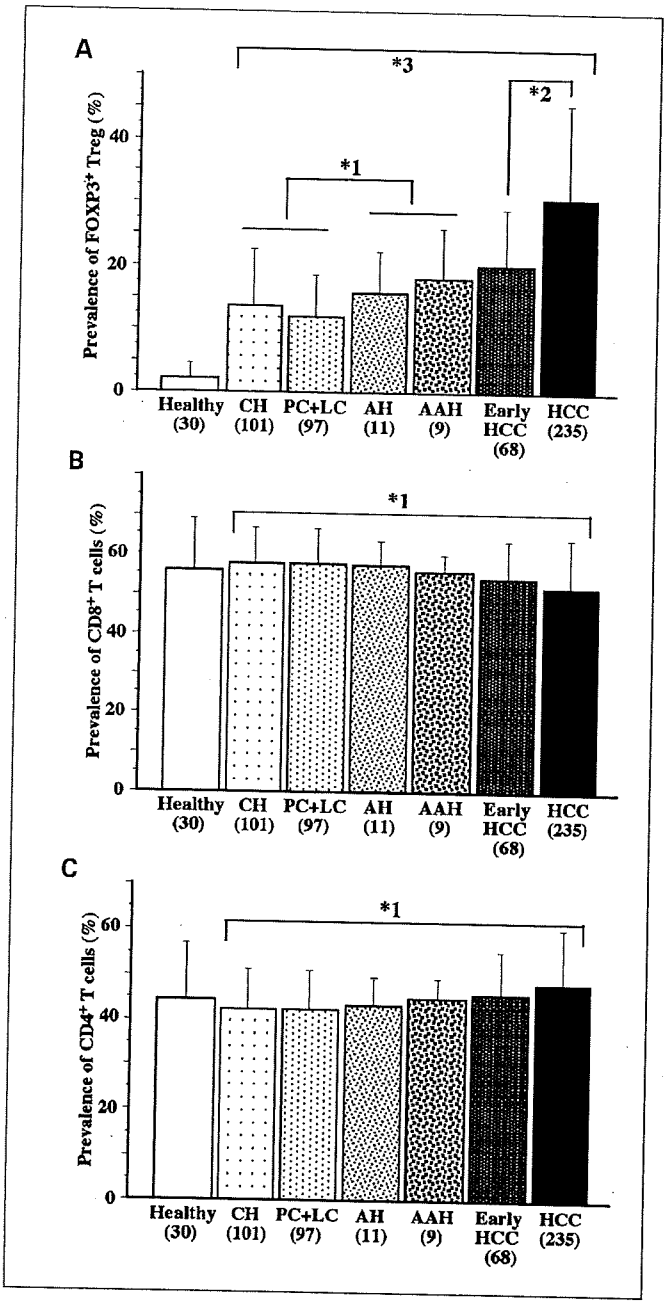

Fig. 3. Increased population of Tregs and decreased population of $CD8^+$ T cells in tumor stroma corresponding to the progression of multistage hepatocarcinogenesis. Prevalence of Tregs among $CD4^+$ Tcells (*A*), prevalence of $CD8^+$ Tcells among total Tcells (*B*), and prevalence of $CD4^+$ Tcells among total T cells (*C*) in HCC, its precursor lesions, and nontumorous liver. Number of cases tested in parentheses; Thin bars, SD. *A*, *1, $P = 0.038$; *2, $P < 0.001$; *3, $P < 0.001$ (Kruskal-Wallis test). *B* and *C*, *1, $P < 0.001$ (Kruskal-Wallis test).

was significantly higher in primary HCC than in IM ($P = 0.003$; Fig. 4A). Also, the prevalence of Tregs in primary hepatic adenocarcinoma was higher than that in metastatic hepatic adenocarcinoma ($P = 0.020$; Fig. 4A). The prevalence of $CD8^+$ T cells was comparable between primary and metastatic tumors.

Hepatitis viral infection and antitumor host immune response. HBV or HCV infection is a risk factor for the development of HCC (2), and it is also reported that these chronic viral infections suppress the host immune response (2). Some investigators have suggested that HCV infection increases ICC development, although this remains to be proven (34). The prevalence of Tregs in nontumorous liver of patients infected with HBV or HCV was significantly higher than in healthy liver (Fig. 4B), even in patients who were in the so-called "carrier" stage, with infection but no detectable manifestations or histologic changes. To investigate whether Tregs affected the development of primary liver tumors, we compared the prevalence of Tregs in nontumorous areas of liver bearing HCC, ICC, or metastatic liver adenocarcinoma among patients with and without hepatitis viral infection. The prevalence of Tregs in nontumorous liver bearing HCC or ICC without any HBV or HCV infection was apparently higher than that in healthy liver (versus HCC, $P < 0.001$; versus ICC, $P < 0.001$; Fig. 4B). In contrast, the prevalence of Tregs in nontumorous liver bearing HCC or ICC with HBV or HCV infection was slightly, but not significantly, higher than that in liver bearing no primary liver tumor with hepatitis virus infection (Fig. 4B). These findings suggest that a further increase of Treg infiltration in nontumorous liver with hepatitis virus infection is not closely correlated with the development of primary liver tumors. An interesting observation was that the prevalence of Tregs in nontumorous liver bearing HCC without HBV or HCV infection was higher than that in healthy liver, and was slightly lower than that in HBV-infected liver (Fig. 4B and C). The prevalence of Tregs in liver infected with HCV was higher than that in liver with HBV infection ($P = 0.016$), and

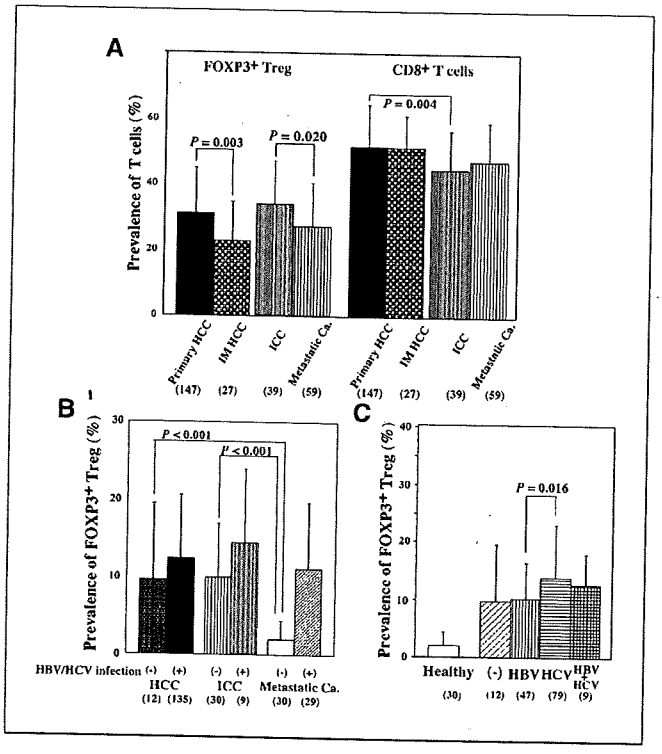

Fig. 4. *A*, prevalence of Tcells in primary liver cancer (HCC and ICC) and metastatic HCC (IM) and adenocarcinoma from colon cancer (metastatic ca.). Left and right columns, the prevalence of Tregs and $CD8^+$ Tcells, respectively. Number of cases tested are in parentheses. *B*, prevalence of Tregs in nontumorous liver of patients bearing HCC, ICC, or metastatic liver cancer, with or without HBV or HBC infection. Number of cases tested in parentheses. *C*, prevalence of Tregs in nontumorous liver of patients bearing HCC. Prevalence of Tregs in nontumorous liver with or without (−) hepatitis B and/or C viral infection were significantly higher than that in healthy controls. Number of cases tested in parentheses.

that in both HBV- and HCV-infected liver was intermediate between that in HBV- and HCV-infected liver. These observations were also recognized in patients with ICC (data not shown).

Discussion

Tumor-infiltrating lymphocytes represent the host immune response to a tumor, and include $CD8^+$ cytotoxic T cells and natural killer cells as positive responders and Tregs as immunosuppressors. There has been no large-scale or clinicopathologic study of Tregs in HCC and tumor-infiltrating lymphocytes in hepatocarcinogenesis. In the present study, we investigated the relationship between host immune response and hepatocarcinogenesis, focusing especially on Treg infiltration. First, we showed the clinicopathologic significance of Tregs among $CD4^+$ T cells infiltrating advanced HCC based on the following findings: (*a*) the prevalence of Tregs in HCC ($n = 235$) was significantly higher ($P < 0.001$) than that in nontumorous liver ($n = 248$), which included healthy liver, NCH, CH, PC, and LC. (*b*) Patients with HCC in the high-Treg group showed a significantly lower survival ratio. Both overall survival (log-rank test, $P = 0.007$) and disease-free survival (log-rank test, $P = 0.015$) were lower than for patients with HCC belonging to the low-Treg group. (*c*) Multivariate analysis revealed that the prevalence of tumor-infiltrating Tregs was an independent prognostic factor, along with Child-Pugh classification and presence of VP, for overall survival and that the prevalence of tumor-infiltrating Tregs and that of IM were independent prognostic factors for disease-free survival. (*d*) The prevalence of tumor-infiltrating Tregs was increased in poorly differentiated HCC (Kruskal-Wallis test; $P < 0.001$). In addition, we found that the prevalence of tumor-infiltrating Tregs increased in a stepwise manner (Kruskal-Wallis test, $P < 0.001$), whereas the prevalence of $CD8^+$ T cells decreased (Kruskal-Wallis test, $P < 0.001$) during the progression of hepatocarcinogenesis. These findings suggest that Treg infiltration was closely correlated with the progression of neoplastic cells in hepatocarcinogenesis. Furthermore, we showed that the prevalence of Tregs was increased in nontumorous liver tissue from patients with primary hepatic tumors, regardless of the presence of hepatitis virus infection or histopathologically evident hepatitis or liver cirrhosis. This indicates that primary hepatic tumors develop in liver, in which Tregs show marked infiltration and immune reactivity is suppressed. This is the first report to show that infiltration of Tregs is closely correlated with the development and progression of hepatocarcinogenesis, and that the prevalence of Tregs is a useful prognostic factor in patients with HCC.

It was reported previously that $CD8^+$ T cells infiltrating tumors are associated with good prognosis (8, 9), and that tumor-infiltrating Treg is increased in a variety of tumors (21–28). A few studies have also investigated the clinicopathologic significance of Treg infiltration (23–25), but conclusions about its correlation with prognosis were contradictory. Marked infiltration of Tregs in cancer stroma was reported to be an unfavorable prognostic factor in ovarian (23) and pancreatic (25) cancers, and was associated with control of tumor progression in head and neck cancers (24). No prognostic influence of Tregs was found in anal squamous cell carcinomas (35). In the present study, using multivariate analyses, we showed that the prevalence of Tregs in HCC was significantly correlated with both overall survival and disease-free survival. A high prevalence of Tregs was closely correlated only with histologic grade among a number of clinicopathologic variables. These findings indicate that the prevalence of tumor-infiltrating $FOXP3^+$ Tregs can be an independent prognostic factor for patients with HCC. In addition to the prevalence of Tregs, our multivariate analysis revealed that among 15 prognostic factors, Child-Pugh classification and the presence of VP and IM were independent indicators of unfavorable overall and disease-free survival, respectively, consistent with previous studies (36, 37). In contrast, infiltration of $CD8^+$ T cells as well as perforin-positive cells (data not shown) in HCC was found to have no prognostic significance. A positive prognostic effect of infiltrating $CD8^+$ T cells has been reported in various solid cancers such as colorectal (8) and ovarian (9) cancer. Only patients bearing HCC with exceptionally marked infiltration of $CD8^+$ T cells were reported to have a good prognosis (10). It is interesting that a negative prognostic effect of $CD8^+$ T cell infiltration has been observed in virus-related tumors, including EB virus–associated nasopharyngeal carcinomas (38) and human papilloma virus–associated anal carcinomas (35). This effect observed in other tumors was not observed in HCC, even though HCC is closely associated with hepatitis virus infection, and might be attributable to an organ-specific immune response.

In established HCC, Treg infiltration might play an important role in tumor progression and clinical behavior by modifying the host immune response. Furthermore, our data showed that the prevalence of Tregs increased in a stepwise manner from viral hepatitis containing CH, PC, and LC, to precursor lesions of AH and AAH, early HCC, and advanced HCC, indicating that Treg infiltration was closely involved in the progression of hepatocarcinogenesis ($P < 0.001$; Fig. 3A). It has been suggested that Tregs suppress the immune response through cell contact–dependent (12–14) or cell contact–independent mechanisms (15, 16), and that immune suppression occurs in several steps (12, 14, 16). Various immune cells could be the targets of Treg suppression, such as $CD8^+$ T cells, $CD4^+CD25^-$ T cells, B cells, natural killer cells, natural killer T-cells, and dendritic cells (12, 14, 16, 39, 40). In this study, the prevalence of $CD8^+$ tumor-infiltrating lymphocytes was found to decrease significantly during hepatocarcinogenesis ($P < 0.001$; Fig. 3B), and this was inversely correlated with Treg infiltration. The group of patients with advanced HCC showing marked Treg infiltration showed a tendency to have a lower prevalence of $CD8^+$ tumor-infiltrating lymphocytes (Table 2A). Thus, it is possible that Tregs contribute to reducing the infiltration of $CD8^+$ T cells during hepatocarcinogenesis. Unitt et al. reported that Tregs isolated from advanced HCC suppressed the proliferation and perforin expression of autologous circulating $CD8^+$ T cells (27).

Persistent viral infection requires host immune suppression. $CD4^+CD25^+$ Tregs have been reported to be linked to the chronicity and progression of viral hepatitis in patients with HBV or HCV infection by down-regulating the hepatitis virus-specific T cell response (41–43). Our present observations confirm marked infiltration of Tregs in the liver of patients infected with HBV or HCV. Regardless of the presence of hepatitis virus infection and histopathologic changes indicative of hepatitis, the prevalence of Tregs in nontumorous liver tissue

of patients bearing HCC was significantly higher than that in healthy liver, but was slightly lower than that in liver with viral hepatitis. It has been suggested that even in patients with HCC of unknown etiology, immunosuppression might have started in the liver before tumor development. In patients with primary hepatic adenocarcinoma, ICC, the prevalence of FOXP3$^+$ Tregs in nontumorous liver without viral infection was also higher than that in healthy liver. These findings suggest that primary hepatic tumors can develop in the liver with a certain degree of Treg infiltration. A subsequent increase of Treg infiltration seemed to accelerate the development of hepatic tumors in patients infected with hepatitis virus, but not to a significant degree. Further studies will be necessary to clarify the threshold of Treg prevalence at which the risk of hepatic tumor development becomes high. The prevalence of Tregs in primary hepatic tumors, both HCC and adenocarcinoma, was significantly higher than that in metastatic hepatic tumors with the corresponding histology. These findings support the hypothesis that the development and progression of primary hepatic tumors involves high accumulation of Tregs.

In conclusion, our data suggest that Tregs play a role in controlling the immune response to HCC from the precursor stage to established cancer, and also that primary hepatic cancers might develop in liver that is immunosuppressed by marked infiltration of Tregs, regardless of the presence of hepatitis viral infection. A high prevalence of Tregs seems to be an indicator of poor prognosis.

Acknowledgments

The authors thank Rie Itoh, Yuko Yamauchi, and Kaoru Onozato for technical assistance.

References

1. Llovet JM, Burroughs A, Bruix J. Hepatocellular carcinoma. Lancet 2003;362:1907–17.
2. Kao JH, Chen DS. Overview of hepatitis B and C viruses. Infectious causes of Cancer. In: Goedert JJ, editor. New Jersey: Humana Press; 2000.
3. Ueno Y, Moriyama M, Uchida T, Arakawa Y. Irregular regeneration of hepatocytes is an important factor in the hepatocarcinogenesis of liver disease. Hepatology 2001;33:357–62.
4. Tsuda H, Hirohashi S, Shimosato Y, Terada M, Hasegawa H. Clonal origin of atypical adenomatous hyperplasia of the liver and clonal identity with hepatocellular carcinoma. Gastroenterology 1988;95:1664–6.
5. Sakamoto M, Hirohashi S, Shimosato Y. Early stages of multistep hepatocarcinogenesis: adenomatous hyperplasia and early hepatocellular carcinoma. Hum Pathol 1991;22:172–8.
6. Saito Y, Kanai Y, Sakamoto M, Saito H, Ishii H, Hirohashi S. Expression of mRNA for DNA methyltransferases and methyl-CpG-binding proteins and DNA methylation status on CpG islands and pericentromeric satellite regions during human hepatocarcinogenesis. Hepatology 2001;33:561–8.
7. Chuma M, Sakamoto M, Yamazaki K, et al. Expression profiling in multistage hepatocarcinogenesis: identification of HSP70 as a molecular marker of early hepatocellular carcinoma. Hepatology 2003;37:198–207.
8. Zhang L, Conejo-Garcia JR, Katsaros D, et al. Intratumoral T cells, recurrence, and survival in epithelial ovarian cancer. N Engl J Med 2003;348:203–13.
9. Naito Y, Saito K, Shiiba K, et al. CD8$^+$ T cells infiltrated within cancer cell nests as a prognostic factor in human colorectal cancer. Cancer Res 1998;58:3491–4.
10. Wada Y, Nakashima O, Kutami R, Yamamoto O, Kojiro M. Clinicopathological study on hepatocellular carcinoma with lymphocytic infiltration. Hepatology 1998;27:407–14.
11. Nakamoto Y, Suda T, Momoi T, Kaneko S. Different procarcinogenic potentials of lymphocyte subsets in a transgenic mouse model of chronic hepatitis B. Cancer Res 2004;64:3326–33.
12. Sakaguchi S. Regulatory T cells: key controllers of immunologic self-tolerance. Cell 2000;101:455–8.
13. Dieckmann D, Plottner H, Berchtold S, Berger T, Schuler G. *Ex vivo* isolation and characterization of CD4$^+$CD25$^+$ T cells with regulatory properties from human blood. J Exp Med 2001;193:1303–10.
14. Shevach EM. CD4$^+$CD25$^+$ suppressor T cells: more questions than answers. Nat Rev Immunol 2002;2:389–400.
15. Chen ML, Pittet MJ, Gorelik L, et al. Regulatory T cells suppress tumor-specific CD8 T cell cytotoxicity through TGF-b signals *in vivo*. Proc Natl Acad Sci U S A 2005;102:419–24.
16. von Boehmer H. Mechanisms of suppression by suppressor T cells. Nat Immunol 2005;6:338–44.
17. Fontenot JD, Rudensky AY. A well adapted regulatory contrivance: regulatory T cell development and the forkhead family transcription factor Foxp3. Nat Immunol 2005;6:331–7.
18. Shimizu JS, Yamazaki S, Sakaguchi S. Induction of tumor immunity by removing CD25$^+$CD4$^+$ T cells: a common basis between tumor immunity and autoimmunity. J Immunol 1999;163:5211–8.
19. Onizuka SI, Tawara J, Shimizu J, Sakaguchi S, Fujita T, Nakayama E. Tumor rejection by *in vivo* administration of anti-CD25 (interleukin-2 receptor a) monoclonal antibody. Cancer Res 1999;59:3128–33.
20. Nishikawa H, Kato T, Tawara I, et al. Accelerated chemically induced tumor development mediated by CD4$^+$CD25$^+$ regulatory T cells in wild-type hosts. Proc Natl Acad Sci U S A 2005;102:9253–7.
21. Woo EY, Chu CS, Goletz TJ, et al. Regulatory CD4$^+$CD25$^+$ T cells in tumors from patients with early-stage non-small lung cancer and late-stage ovarian cancer. Cancer Res 2001;61:4766–72.
22. Liyanage UK, Moore TT, Joo HG, et al. Prevalence of regulatory T cells is increased in peripheral blood and tumor microenvironment of patients with pancreas or breast adenocarcinoma. J Immunol 2002;169:2756–61.
23. Curiel TJ, Coukos G, Zou L, et al. Specific recruitment of regulatory T cells in ovarian carcinoma fosters immune privilege and predicts reduced survival. Nat Med 2004;10:942–9.
24. Badoual C, Hans S, Rodriguez J, et al. Prognostic value of tumor-infiltrating CD4$^+$ T-cell subpopulations in head and neck cancers. Clin Cancer Res 2006;12:465–72.
25. Hiraoka N, Onozato K, Kosuge T, Hirohashi S. Prevalence of FOXP3$^+$ regulatory T cells increases during the progression of pancreatic ductal adenocarcinoma and its premalignant lesions. Clin Cancer Res 2006;12:5423–34.
26. Ormandy LA, Hillemann T, Wedemeyer H, Manns MP, Greten TF, Korangy F. Increased populations of regulatory T cells in peripheral blood of patients with hepatocellular carcinoma. Cancer Res 2005;65:2457–64.
27. Unitt E, Rushbrook SM, Marshall A, et al. Compromised lymphocytes infiltrate hepatocellular carcinoma: the role of T-regulatory cells. Hepatology 2005;41:722–30.
28. Yang XH, Yamagiwa S, Ichida T, et al. Increase of CD4$^+$CD25$^+$ regulatory T-cells in the liver of patients with hepatocellular carcinoma. J Hepatol 2006;45:254–62.
29. Ruprecht CR, Gattorno M, Ferlito F, et al. Coexpression of CD25 and CD27 identifies Foxp3$^+$ regulatory T cells in inflamed synovia. J Exp Med 2005;201:1793–803.
30. Hirohashi S, Ishak KG, Kojiro M, et al. Hepatocellular carcinoma. In: Hamilton SR, Aaltonen LA, editors. Pathology and genetics of tumors of the digestive system. Lyon: IARC Press; 2000. p. 159–72.
31. Greene FL, Page DL, Fleming ID, et al. AJCC cancer staging manual. 6th ed. Chicago: Springer; 2002. p. 131–44.
32. Ishak K, Baptista A, Bianchi L, et al. Histological grading and staging of chronic hepatitis. J Hepatol 1995;22:696–9.
33. Takahashi Y, Akishima-fukasawa Y, Kobayashi N, et al. Prognostic value of tumor architecture, tumor-associated vascular characteristics, and expression of angiogenic molecules in pancreatic endocrine tumors. Clin Cancer Res 2007;13:187–96.
34. Okuda K, Nakanuma Y, Miyazaki M. Cholangiocarcinoma: recent progress. Part 1: Epidemiology and etiology. J Gastroenterol Hepatol 2002;17:1049–55.
35. Grabenbauer GG, Lahmer G, Distel L, Niedobitek G. Tumor-infiltrating cytotoxic T cells but not regulatory T cells predict outcome in anal squamous cell carcinoma. Clin Cancer Res 2006;12:3355–60.
36. Franco D, Capussotti L, Smadja C, et al. Resection of hepatocellular carcinomas: results in 72 European patients with cirrhosis. Gastroenterology 1990;98:733–8.
37. Izumi R, Shimizu K, Ii T, et al. Prognostic factors of hepatocellular carcinoma in patients undergoing hepatic resection. Gastroenterology 1994;106:720–7.
38. Oudejans JJ, Harijadi H, Kummer JA, et al. High numbers of granzyme B/CD8-positive tumor-infiltrating lymphocytes in nasopharyngeal carcinoma biopsies predict rapid fatal outcome in patients treated with curative intent. J Pathol 2002;198:468–75.
39. Ghiringhelli F, Menard C, Terme M, et al. CD4$^+$CD25$^+$ regulatory T cells inhibit natural killer cell functions in a transforming growth factor-β-dependent manner. J Exp Med 2005;202:1075–85.
40. Tadokoro CE, Shakhar G, Shen S, et al. Regulatory T cells inhibit stable contacts between CD4$^+$ T cells and dendritic cells *in vivo*. J Exp Med 2006;203:505–11.
41. Cabrera R, Tu Z, Xu R, et al. An immunomodulatory role for CD4$^+$CD25$^+$ regulatory T lymphocytes in hepatitis C virus infection. Hepatology 2004;40:1062–73.
42. Stoop JN, van der Molen RG, Baan CC, et al. Regulatory T cells contribute to the impaired immune response in patients with chronic hepatitis B virus infection. Hepatology 2005;41:771–8.
43. Xu D, Fu J, Jin L, et al. Circulating and liver resident CD4$^+$CD25$^+$ regulatory T cells actively influence the antiviral immune response and disease progression in patients with hepatitis B. J Immunol 2006;177:739–47.

Adiponectin inhibits colorectal cancer cell growth through the AMPK/mTOR pathway

MICHIKO SUGIYAMA[1], HIROKAZU TAKAHASHI[1], KUNIHIRO HOSONO[1], HIROKI ENDO[1], SHINGO KATO[1], KYOKO YONEDA[1], YUICHI NOZAKI[1], KOJI FUJITA[1], MASATO YONEDA[1], KOICHIRO WADA[2], HITOSHI NAKAGAMA[3] and ATSUSHI NAKAJIMA[1]

[1]Division of Gastroenterology, Yokohama City University School of Medicine, 3-9 Fuku-ura, Kanazawa-ku, Yokohama; [2]Department of Pharmacology, Graduate School of Dentistry, Osaka University, 1-8 Yamadaoka, Suita, Osaka; [3]Biochemistry Division, National Cancer Center Research Institute, 1-1 Tsukiji 5-chome, Chuo-ku, Tokyo, Japan

Received July 2, 2008; Accepted September 25, 2008

DOI: 10.3892/ijo_00000156

Abstract. Adiponectin is a peptide hormone secreted by adipose tissue. It is a key hormone responsible for insulin sensitization, and its circulating level is inversely associated with abdominal obesity. Recent studies have shown that a reduced plasma adiponectin level is significantly correlated with the risk of various cancers. However, there are few studies regarding the association of adiponectin and colorectal cancer. To address this issue, we investigated the effect of adiponectin on colorectal cancer cells. Three colorectal cancer cell lines express both AdipoR1 and AdipoR2 receptors. MTT assay revealed that adiponectin inhibited human colorectal cancer cell growth. Furthermore, Western blot analysis revealed that adiponectin activated adenosine monophosphate-activated protein kinase (AMPK) and suppressed mammalian target of rapamycin (mTOR) pathways. Selective AMPK inhibitor compound C abrogated the inhibitory effect of adiponectin on cell growth. Our results clearly demonstrate the novel findings that adiponectin inhibits colorectal cancer cell growth via activation of AMPK, thereby down-regulating the mTOR pathway.

Introduction

Colorectal cancer (CRC) is one of the most common malignancies. Obesity, especially visceral obesity, has been reported to be associated with CRC (1,2). Adipose tissue is not only a fat storage organ, but it secretes several bioactive substances known as adipocytokines (3,4). Adiponectin is secreted from adipocytes and is a key hormone responsible for insulin sensitization (5-12). Its plasma level is dramatically decreased in patients with obesity and type 2 diabetes mellitus (DM) (4,5,13). Since both obesity and type 2 DM have been reported to be associated with an elevated risk of CRC (14), it is speculated that the plasma level of adiponectin may be related to the risk of CRC. However, several contradictory results have been reported from human clinical studies on the relationship between the plasma levels of adiponectin and the risk of CRC (15,16).

It is well known that the adiponectin receptor exists in two isoforms: adiponectin receptor 1 (AdipoR1) and 2 (AdipoR2) (17). These receptors mediate cellular functions by activating intracellular signaling pathways (17). The molecular pathways downstream of AdipoRs remain to be fully elucidated, but studies in metabolically-responsive cells have shown that activation of the pleiotropic adenosine monophosphate-activated protein kinase (AMPK) is involved in the signaling cascade downstream of adiponectin receptors (18,19). AMPK plays a key role in the regulation of energy homeostasis and acts as a 'metabolic sensor' to regulate adenosine triphosphate (ATP) concentrations (20). It is also associated with cell growth; phosphorylated AMPK suppresses mammalian target of rapamycin (mTOR) signaling pathway (21,22). mTOR plays a central role in the regulation of cell proliferation, growth, differentiation, migration and survival (23-26), and may be abnormally regulated in tumors (23,27-29). The 70-kDa ribosomal protein S6 kinase (p70S6K) and S6 ribosomal protein (S6P) are part of the signaling cascade downstream of mTOR; they are activated via phosphorylation by mTOR (28,30,31). Non-cleaved adiponectin (full-length adiponectin; f-adiponectin) and proteolytically-cleaved adiponectin containing a C-terminal globular region (globular adiponectin; g-adiponectin) were reported to have different affinities to AdipoR1 and AdipoR2 (17). In this study, we only examined the g-adiponectin because this isoform binds both receptors, while f-adiponectin has low affinity to AdipoR1 (17), and it exerts more potent effect than f-adiponectin (5). However, the expression levels of AdipoR1 and AdipoR2, the affinity of the different forms of

Correspondence to: Dr Atsushi Nakajima, Division of Gastroenterology, Yokohama City University School of Medicine, 3-9 Fuku-ura, Kanazawa-ku, Yokohama, Japan
E-mail: nakajima-tky@umin.ac.jp

Key words: adiponectin, colorectal cancer, cell growth, AdipoR1/AdipoR2, adenosine monophosphate-activated protein kinase

adiponectin to those receptors, and the associated intracellular signaling pathways in the colorectum remain unclear. In this study, we investigated the effect of adiponectin on cell growth and the intracellular signaling pathway involved in CRC cell lines.

Materials and methods

Reagents and antibodies. Human globular adiponectin was purchased from BioVendor Laboratory Medicine Inc. (Brno, Czech Republic). Compound C was purchased from Calbiochem (La Jolla, CA) and 3-(4,5-dimethyl-thiazol-2-yl)-2,5-diphenyl tetrazolium bromide (MTT) was purchased from Sigma Chemical Co. (St. Louis, MO). Anti-total and -phosphorylated (Thr172) AMPK, anti-total and -phosphorylated (Ser2448) mTOR, anti-total and -phosphorylated (Thr421/Ser424) p70S6 kinase, anti-total and -phosphorylated (Ser240/244) S6 ribosomal protein, and anti-rabbit horseradish-peroxidase-conjugated IgG antibodies were obtained from Cell Signaling Technology, Inc. (Beverly, MA). Anti-AdipoR1 (C-14), anti-AdipoR2 (N-19), and anti-goat horseradish-peroxidase-conjugated IgG antibodies were from Santa Cruz Biotechnology, Inc. (Santa Cruz, CA). Anti-glyceraldehyde-3-phosphate dehydrogenase (G3PDH) antibody was from Trevigen, Inc. (Gaithersburg, MD).

Cell lines. The human colon adenocarcinoma cell lines, HT-29, Lovo, and HCT116 were used for this study. Lovo was obtained from Health Science Research Resources Bank (Osaka, Japan), while HT-29 and HCT116 were obtained from American Type Culture Collection (Manassas, VA). HCT116 and HT-29 were cultured in McCoy's 5A, and Lovo was cultured in Ham's F12, supplemented with 10% FBS, penicillin (100 U/ml) and streptomycin (100 μg/ml) (all from Invitrogen, Carlsbad, CA) at 37°C under a humidified atmosphere of 5% CO_2.

Western blot analysis. Cultured cells treated with the test compound for indicated time periods were rinsed with phosphate-buffer saline (PBS). For obtaining the total cell extracts, cells were harvested in lysis buffer (50 mM Tris-HCl, 100 mM NaCl, 5 mM EDTA, 1% TritonX-100) containing a cocktail of protease inhibitors (Sigma). The lysates were incubated on ice for 30 min and centrifuged at 15,000 rpm. Protein concentrations were determined using the Bio-Rad Protein Assay Reagent (Bio-Rad, Richmond, CA). Proteins were separated by SDS/PAGE (7.5-12.5% gels) and transferred onto a Hybond-P PVDF membrane (Amersham Biosciences, Little Chalfont, UK). After the transfer, the membranes were blocked with Blocking One-P (Nacalai Tesque, Kyoto, Japan) and probed with the primary antibodies specified below. Horseradish-peroxidase-conjugated secondary antibodies and the ECL detection kit (Amersham Biosciences, Little Chalfont, UK) were used for the detection of specific proteins. Images were captured and analyzed by LAS-3000 imaging system (Fujifilm, Tokyo, Japan).

Cell growth assay. Cells were seeded in 96-well, flat-bottom microtiter plates at a density of $5x10^3$ cells per well and incubated in medium containing 1% FBS. After 24 h, the complete medium was replaced with test medium for 24 h at 37°C. After incubating the plates for an additional 4 h with MTT solution (0.5%), sodium dodecylsulfate was added to a final concentration of 10% and absorbance at 595 nm was determined for each well using a microplate reader (Model 550; Bio-Rad). Three independent experiments were carried out for each cell line. Annexin V-FITC and PI double staining with the Annexin V-FITC apoptosis detection kit I (Becton-Dickinson, San Jose, CA, USA) followed by FACScan flow cytometry (Becton-Dickinson) was used to identify apoptotic cells. Cell fluorescence was measured with a FACScan flow cytometer from BD Biosciences (San Jose, CA, USA). Dual parameter cytometric data were analyzed by using CellQuest software from BD Biosciences. Apoptosis measures were performed in triplicate.

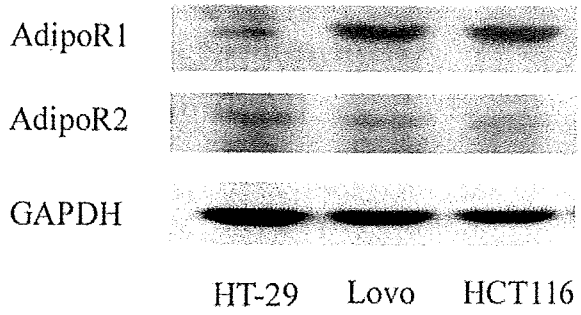

Figure 1. Expression of adiponectin receptors in colorectal cancer cells. Western blot analysis revealed that three kinds of colorectal cancer cell lines HCT116, HT-29 and Lovo cells, expressed both AdipoR1 and AdipoR2 receptors.

Statistical analysis. All results are expressed as mean ± SEM. Statistical analyses were performed using Student's t-test after analysis of variance (ANOVA). The results were considered to be statistically significant at $p<0.05$.

Results

Expression of adiponectin receptors on colorectal cancer cells. Western blot analysis revealed that three kinds of colorectal cancer cell lines, HCT116, HT-29 and Lovo, expressed both AdipoR1 and AdipoR2 receptors (Fig. 1). In HT-29, weak expressions of both of AdipoRs were observed. In Lovo and HCT116, strong expression of AdipoR1, and weak expression of AdipoR2 were observed.

Globular adiponectin (g-adiponectin) inhibited human colorectal cancer cell growth. To determine the effect of g-adiponectin on colorectal cancer cell growth, MTT assay was performed using HCT116, HT-29 and Lovo cells. To reduce the effect of adiponectin in serum, all experiments were conducted using the culture medium containing 1% FBS. G-adiponectin significantly inhibited colorectal cancer cell growth in all examined cells in a dose-dependent manner (Fig. 2).

G-adiponectin up-regulates AMPK activity in colorectal cancer cells. The effect of g-adiponectin on the phosphorylation of

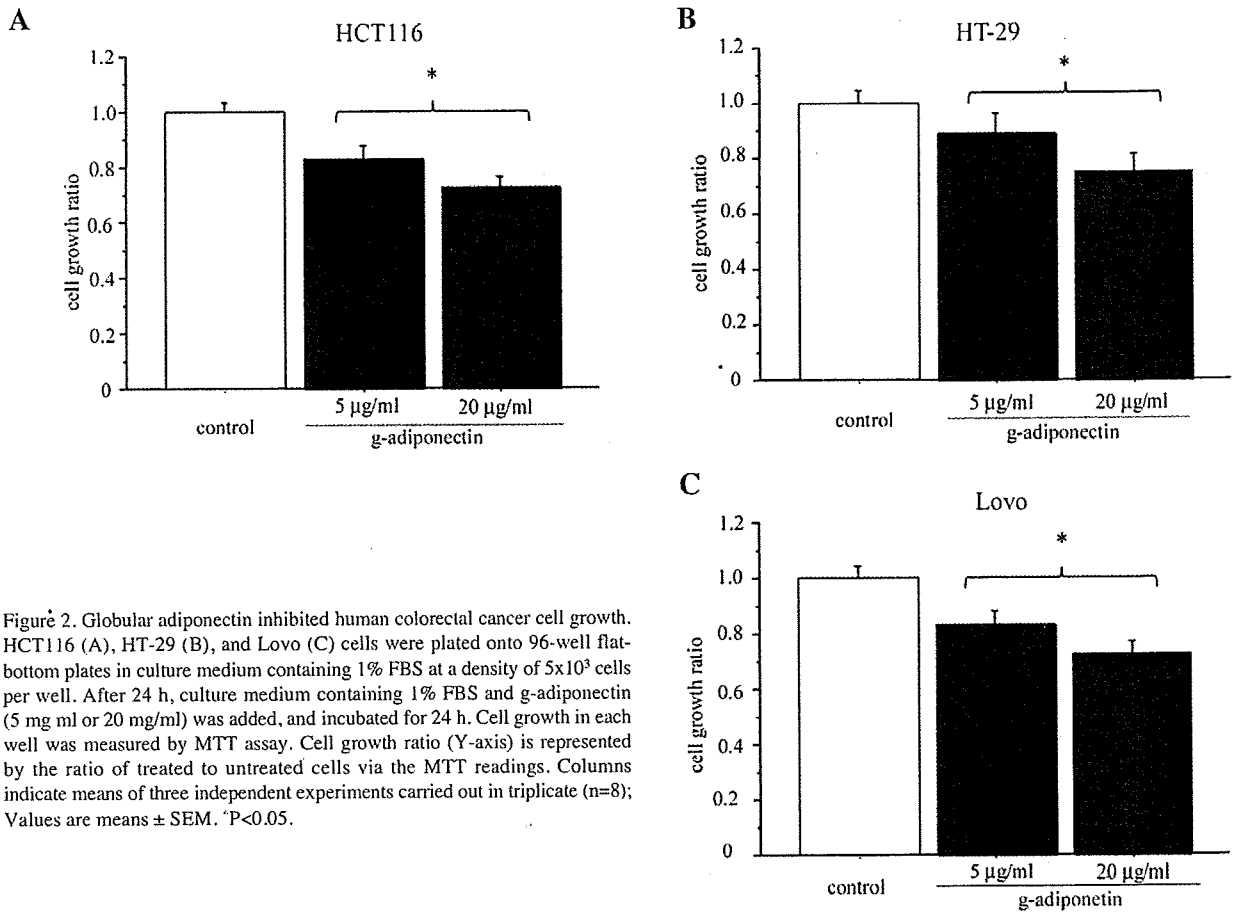

Figure 2. Globular adiponectin inhibited human colorectal cancer cell growth. HCT116 (A), HT-29 (B), and Lovo (C) cells were plated onto 96-well flat-bottom plates in culture medium containing 1% FBS at a density of $5x10^3$ cells per well. After 24 h, culture medium containing 1% FBS and g-adiponectin (5 mg ml or 20 mg/ml) was added, and incubated for 24 h. Cell growth in each well was measured by MTT assay. Cell growth ratio (Y-axis) is represented by the ratio of treated to untreated cells via the MTT readings. Columns indicate means of three independent experiments carried out in triplicate (n=8); Values are means ± SEM. *P<0.05.

AMPK and mTOR signaling pathway was examined. Western blot analysis revealed that g-adiponectin significantly phosphorylated AMPK and its effect on AMPK phosphorylation was maximal at 6 h after treatment (Fig. 3A). We also observed the significant phosphorylation of mTOR, p70S6K, and S6 proteins by the treatment with g-adiponectin (Fig. 3B-D). These results suggest that g-adiponectin inhibits colorectal cancer cell growth via AMPK activation and mTOR signaling pathway suppression. Selective AMPK inhibitor compound C reversed the g-adiponectin induced cell growth inhibition in HCT116 colorectal cancer cells, as detected by MTT assay (Fig. 3E). This indicates that g-adiponectin-induced cell growth inhibition is mediated by activation of AMPK.

G-adiponectin has no effect on apoptosis. The effect of g-adiponectin on apoptosis in HCT116 and HT-29 was evaluated using annexin V-FITC and PI double staining. There was no apoptotic effect in HCT116 and HT-29 treated with 5 μg/ml g-adiponectin or 20 μg/ml g-adiponectin in basal medium containing 1% FBS (Fig. 4).

Discussion

The association of low plasma adiponectin level and cancer risk was previously reported (32-35). However, there are few studies regarding the association of adiponectin and colorectal cancer (15,36). In the present study, we demonstrated both of the AdipoR expression levels and g-adiponectin activation of the AMPK, resulting in the suppression of mTOR signaling pathway in colorectal cancer cell lines. Our recent study demonstrated that AdipoRs were expressed in normal colon epithelial and colorectal cancer cells in human (37). In this study, three kinds of colorectal cancer cell lines HCT116, HT-29 and Lovo cells were shown to express AdipoRs. Furthermore, we clearly demonstrated that globular adiponectin inhibited colorectal cancer cell growth and activated AMPK, while selective AMPK inhibitor compound C reversed the effect of g-adiponectin-induced cell growth inhibition, which indicates that g-adiponectin inhibits cell growth via regulation of AMPK. mTOR is one of the enzymes downstream of AMPK. AMPK activation acts as an inhibitor of mTOR pathway and suppresses tumor development (38,39). In this study, we demonstrated that g-adiponectin suppressed the mTOR pathway following the activation of AMPK. These results suggest that g-adiponectin suppresses cancer cell growth through AMPK activation and subsequent inhibition of mTOR pathway. However, the mechanisms through which adiponectin affects cancer cells are not completely elucidated, thus there is a possibility that suppression of mTOR pathway by adiponectin is mediated through other enzymes (40,41). Further studies are needed to evaluate the molecular pathways downstream of each AdipoR.

In conclusion, this study clearly demonstrates the novel findings that g-adiponectin inhibits colorectal cancer cell

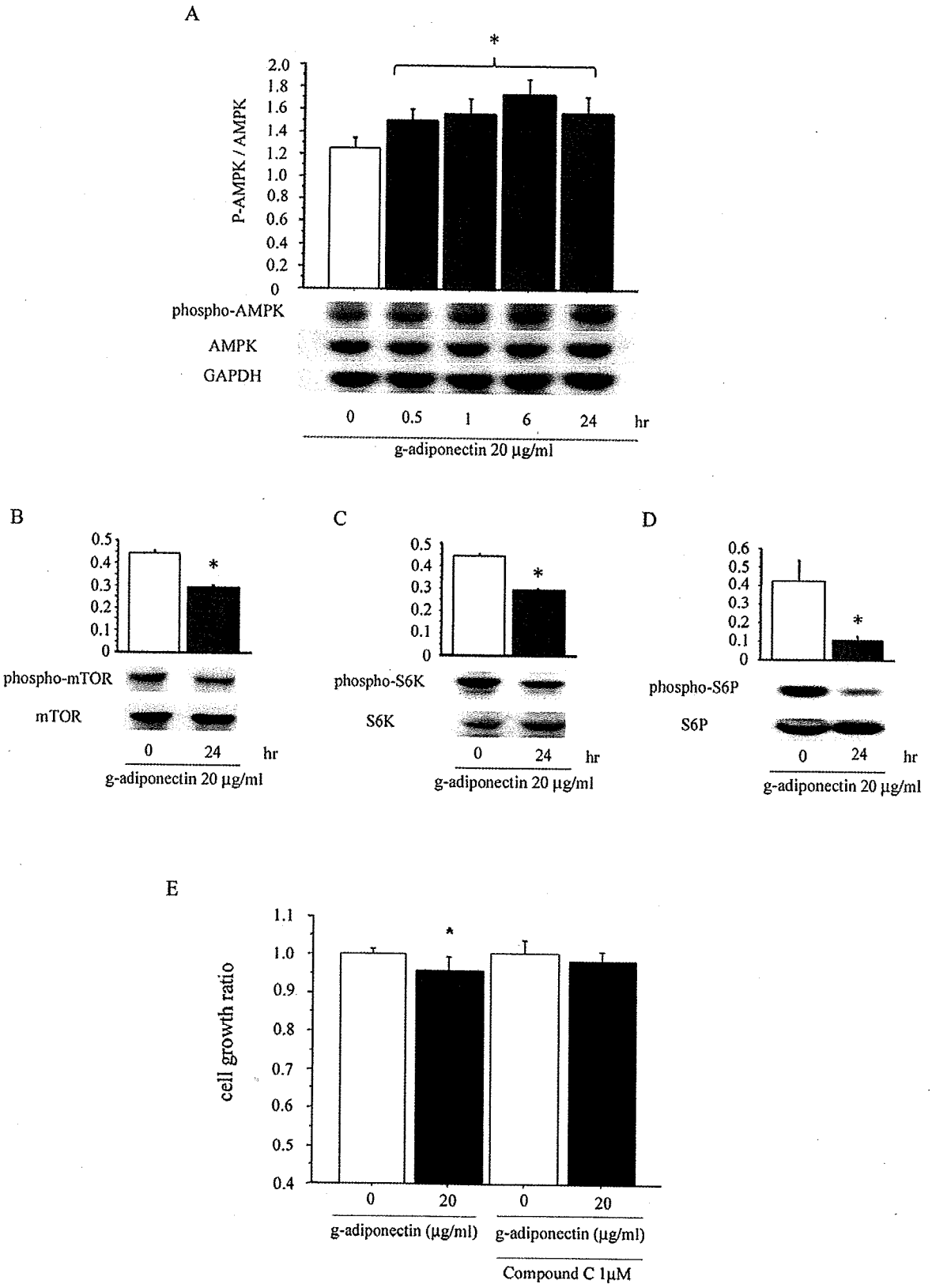

Figure 3. G-adiponectin up-regulates AMPK activity in colorectal cancer cell and selective AMPK inhibitor compound C reversed the g-adiponectin-induced cell growth. Western blot analysis was performed. HCT116 cells were treated with culture medium containing 1% FBS and g-adiponectin (20 μg/ml) for 24 h. After harvesting, cells were lysed and prepared for immunoblot analysis. (A) G-adiponectin increases AMPK phosphorylation and its effect on AMPK phosphorylation was maximal at 6 h after treatment. (B-D) G-adiponectin reduced phosphorylation of mTOR, p70S6K and S6P in HCT116 cells. Western blot analysis was performed in triplicate. Values are means ± SEM. *P<0.05. (E) To confirm the effect of adiponectin-induced growth inhibition via AMPK, HCT116 incubated in culture medium containing 1% FBS and adiponectin (20 μg/ml) alone or with the addition of compound C (1 μM) for 24 h were used for MTT assay. Columns indicate means of four independent experiments carried out in triplicate (n=8); Values are means ± SEM. *P<0.05.

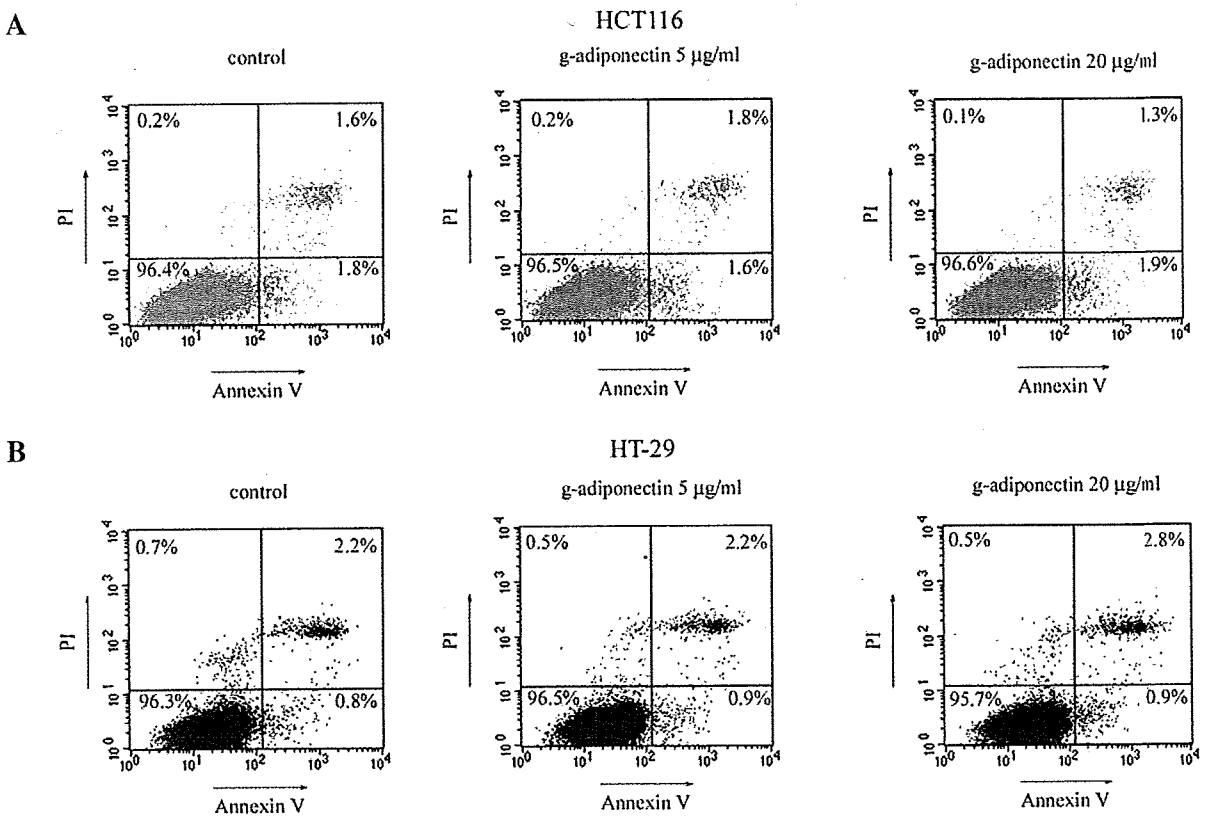

Figure 4. G-adiponectin has no effect on apoptosis. The apoptotic effect of g-adiponectin in HCT116 (A) and HT-29 (B) colorectal cancer cells incubated with culture medium containing 1% FBS and g-adiponectin (5 μg/ml or 20 μg/ml) were evaluated via annexin V-FITC and PI double staining. Apoptosis measures were performed in triplicate.

growth through the activation of AMPK and subsequent suppression of mTOR pathway. This may be a key step in the elucidation of the effect of adiponectin on colorectal cancer. Further studies are required to elucidate the function of adiponectin in colorectal cancer.

Acknowledgements

We thank Machiko Hiraga and Yuko Sato for their technical assistance. This work was supported in part by a Grant-in-Aid for research on the Third Term Comprehensive Control Research for Cancer from the Ministry of Health, Labour and Welfare, Japan to A.N., a grant from the National Institute of Biomedical Innovation (NBIO) to A.N., a grant from the Ministry of Education, Culture, Sports, Science and Technology, Japan (KIBAN-B) to A.N, and a research grant from the Princess Takamatsu Cancer Research Fund to A.N.

References

1. Pischon T, Lahmann PH, Boeing H, Friedenreich C, Norat T, Tjønneland A, Halkjaer J, Overvad K, Clavel-Chapelon F, Boutron-Ruault MC, Guernec G, Bergmann MM, Linseisen J, Becker N, Trichopoulou A, Trichopoulos D, Sieri S, Palli D, Tumino R, Vineis P, Panico S, Peeters PH, Bueno-de-Mesquita HB, Boshuizen HC, van Guelpen B, Palmqvist R, Berglund G, Gonzalez CA, Dorronsoro M, Barricarte A, Navarro C, Martinez C, Quirós JR, Roddam A, Allen N, Bingham S, Khaw KT, Ferrari P, Kaaks R, Slimani N and Riboli E: Body size and risk of colon and rectal cancer in the European Prospective Investigation Into Cancer and Nutrition (EPIC). J Natl Cancer Inst 98: 920-931, 2006.
2. Takahash H, Yoneda K, Tomimoto A, Endo H, Fujisawa T, Iida H, Mawatari H, Nozaki Y, Ikeda T, Akiyama T, Yoneda M, Inamori M, Abe Y, Saito S, Nakajima A and Nakagama H: Life style-related diseases of the digestive system: colorectal cancer as a life style-related disease: from carcinogenesis to medical treatment. J Pharmacol Sci 105: 129-132, 2007.
3. Spranger J, Kroke A, Möhlig M, Bergmann MM, Ristow M, Boeing H and Pfeiffer AF: Adiponectin and protection against type 2 DM. Lancet 361: 226-228, 2003.
4. Hotta K, Funahashi T, Arita Y, Takahashi M, Matsuda M, Okamoto Y, Iwahashi H, Kuriyama H, Ouchi N, Maeda K, Nishida M, Kihara S, Sakai N, Nakajima T, Hasegawa K, Muraguchi M, Ohmoto Y, Nakamura T, Yamashita S, Hanafusa T and Matsuzawa Y: Plasma concentrations of a novel, adipose-specific protein, adiponectin, in type 2 diabetic patients. Arterioscler Thromb Vasc Biol 20: 1595-1599, 2000.
5. Yamauchi T, Kamon J, Waki H, Terauchi Y, Kubota N, Hara K, Mori Y, Ide T, Murakami K, Tsuboyama-Kasaoka N, Ezaki O, Akanuma Y, Gavrilova O, Vinson C, Reitman ML, Kagechika H, Shudo K, Yoda M, Nakano Y, Tobe K, Nagai R, Kimura S, Tomita M, Froguel P and Kadowaki T: The fat-derived hormone adiponectin reverses insulin resistance associated with both lipoatrophy and obesity. Nat Med 7: 941-946, 2001.
6. Berg AH, Combs TP, Du X, Brownlee M and Scherer PE: The adipocyte-secreted protein Acrp30 enhances hepatic insulin action. Nat Med 7: 947-953, 2001.
7. Kubota N, Terauchi Y, Yamauchi T, Kubota T, Moroi M, Matsui J, Eto K, Yamashita T, Kamon J, Satoh H, Yano W, Froguel P, Nagai R, Kimura S, Kadowaki T and Noda T: Disruption of adiponectin causes insulin resistance and neointimal formation. J Biol Chem 277: 25863-25866, 2002.
8. Maeda N, Shimomura I, Kishida K, Nishizawa H, Matsuda M, Nagaretani H, Furuyama N, Kondo H, Takahashi M, Arita Y, Komuro R, Ouchi N, Kihara S, Tochino Y, Okutomi K, Horie M, Takeda S, Aoyama T, Funahashi T and Matsuzawa Y: Diet-induced insulin resistance in mice lacking adiponectin/ACRP30. Nat Med 8: 731-737, 2002.

9. Yamauchi T, Kamon J, Minokoshi Y, Ito Y, Waki H, Uchida S, Yamashita S, Noda M, Kita S, Ueki K, Eto K, Akanuma Y, Froguel P, Foufelle F, Ferre P, Carling D, Kimura S, Nagai R, Kahn BB and Kadowaki T: Adiponectin stimulates glucose utilization and fatty-acid oxidation by activating AMP-activated protein kinase. Nat Med 8: 1288-1295, 2002.
10. Tomas E, Tsao TS, Saha AK, Murrey HE, Zhang Cc C, Itani SI, Lodish HF and Ruderman NB: Enhanced muscle fat oxidation and glucose transport by ACRP30 globular domain: acetyl-CoA carboxylase inhibition and AMP-activated protein kinase activation. Proc Natl Acad Sci USA 99: 16309-16313, 2002.
11. Yamauchi T, Kamon J, Waki H, Imai Y, Shimozawa N, Hioki K, Uchida S, Ito Y, Takakuwa K, Matsui J, Takata M, Eto K, Terauchi Y, Komeda K, Tsunoda M, Murakami K, Ohnishi Y, Naitoh T, Yamamura K, Ueyama Y, Froguel P, Kimura S, Nagai R and Kadowaki T: Globular adiponectin protected ob/ob mice from diabetes and apoE deficient mice from atherosclerosis. J Biol Chem 278: 2461-2468, 2003.
12. Tilg H and Hotamisligil GS: Non-alcoholic fatty liver disease: cytokine-adipokine interplay and regulation of insulin resistance. Gastroenterology 131: 934-945, 2006.
13. Hu E, Liang P and Spiegelman BM: AdipoQ is a novel adipose-specific gene dysregulated in obesity. J Biol Chem 271: 10697-10703, 1996.
14. Giovannucci E and Michaud D: The role of obesity and related metabolic disturbances in cancers of the colon, prostate, and pancreas. Gastroenterology 132: 2208-2225, 2007.
15. Wei EK, Giovannucci E, Fuchs CS, Willett WC and Mantzoros CS: Low plasma adiponectin levels and risk of CRC in men: a prospective study. J Natl Cancer Inst 97: 1688-1694, 2005.
16. Lukanova A, Söderberg S, Kaaks R, Jellum E and Stattin P: Serum adiponectin is not associated with risk of colorectal cancer. Cancer Epidemiol Biomarkers Prev 15: 401-402, 2006.
17. Yamauchi T, Kamon J, Ito Y, Tsuchida A, Yokomizo T, Kita S, Sugiyama T, Miyagishi M, Hara K, Tsunoda M, Murakami K, Ohteki T, Uchida S, Takekawa S, Waki H, Tsuno NH, Shibata Y, Terauchi Y, Froguel P, Tobe K, Koyasu S, Taira K, Kitamura T, Shimizu T, Nagai R and Kadowaki T: Cloning of adiponectin receptors that mediate antidiabetic metabolic effects. Nature 423: 762-769, 2003.
18. Goldstein BJ and Scalia R: Adiponectin: a novel adipokine linking adipocytes and vascular function. J Clin Endocrinol Metab 89: 2563-2568, 2004.
19. Luo Z, Saha AK, Xiang X and Ruderman NB: AMPK, the metabolic syndrome and cancer. Trends Pharmacol Sci 26: 69-76, 2005.
20. Long YC and Zierath JR: AMP-activated protein kinase signaling in metabolic regulation. J Clin Invest 116: 1776-1783, 2006.
21. Bolster DR, Crozier SJ, Kimball SR and Jefferson LS: AMP-activated protein kinase suppresses protein synthesis in rat skeletal muscle through downregulated mTOR signaling. J Biol Chem 277: 23977-23980, 2002.
22. Krause U, Bertrand L and Hue L: Control of p70 ribosomal protein S6 kinase and acetyl-CoA carboxylase by AMP-activated protein kinase and protein phosphatases in isolated hepatocytes. Eur J Biochem 269: 3751-3759, 2002.
23. Vogt PK: PI 3-kinase, mTOR, protein synthesis and cancer. Trends Mol Med 7: 482-484, 2001.
24. Valentinis B and Baserga R: IGF-I receptor signalling in transformation and differentiation. Mol Pathol 54: 133-137, 2001.
25. Oldham S and Hafen E: Insulin/IGF and target of rapamycin signaling: a TOR de force in growth control. Trends Cell Biol 13: 79-85, 2003.
26. Jacinto E and Hall MN: Tor signalling in bugs, brain and brawn. Nat Rev Mol Cell Biol 4: 117-126, 2003.
27. Dancey JE: Clinical development of mammalian target of rapamycin inhibitors. Hematol Oncol Clin North Am 16: 1101-1114, 2002.
28. Huang S and Houghton PJ: Targeting mTOR signaling for cancer therapy. Curr Opin Pharmacol 3: 371-377, 2003.
29. Philp AJ, Campbell IG, Leet C, Vincan E, Rockman SP, Whitehead RH, Thomas RJ and Phillips WA: The phosphatidylinositol 3'-kinase p85alpha gene is an oncogene in human ovarian and colon tumors. Cancer Res 61: 7426-7429, 2001.
30. Fingar DC, Richardson CJ, Tee AR, Cheatham L, Tsou C and Blenis J: mTOR controls cell cycle progression through its cell growth effectors S6K1 and 4E-BP1/eukaryotic translation initiation factor 4E. Mol Cell Biol 24: 200-216, 2004.
31. Hardie DG: New roles for the LKB1→AMPK pathway. Curr Opin Cell Biol 17: 167-173, 2005.
32. Mantzoros C, Petridou E, Dessypris N, Chavelas C, Dalamaga M, Alexe DM, Papadiamantis Y, Markopoulos C, Spanos E, Chrousos G and Trichopoulos D: Adiponectin and breast cancer risk. J Clin Endocrinol Metab 89: 1102-1107, 2004.
33. Miyoshi Y, Funahashi T, Kihara S, Taguchi T, Tamaki Y, Matsuzawa Y and Noguchi S: Association of serum adiponectin levels with breast cancer risk. Clin Cancer Res 9: 5699-5704, 2003.
34. Petridou E, Mantzoros C, Dessypris N, Koukoulomatis P, Addy C, Voulgaris Z, Chrousos G and Trichopoulos D: A case-control study in Greece. J Clin Endocrinol Metab 88: 993-997, 2003.
35. Petridou E, Mantzoros C, Dessypris N, Koukoulomatis P, Addy C, Voulgaris Z, Chrousos G and Trichopoulos D: Circulating adiponectin and endometrial cancer risk. J Clin Endocrinol Metab 89: 1160-1163, 2004.
36. Otake S, Takeda H, Suzuki Y, Fukui T, Watanabe S, Ishihama K, Saito T, Togashi H, Nakamura T, Matsuzawa Y and Kawata S: Association of visceral fat accumulation and plasma adiponectin with colorectal adenoma: evidence for participation of insulin resistance. Clin Cancer Res 11: 3642-3646, 2005.
37. Yoneda K, Tomimoto A, Endo H, Iida H, Sugiyama M, Takahashi H, Mawatari H, Nozaki Y, Fujita K, Yoneda M, Inamori M, Nakajima N, Wada K, Nagashima Y, Nakagama H, Uozaki H, Fukayama M and Nakajima A: Expression of adiponectin receptors, AdipoR1 and AdipoR2, in normal colon epithelium and colon cancer tissue. Oncol Rep 20: 479-483, 2008.
38. Schmelzle T and Hall MN: TOR, a central controller of cell growth. Cell 103: 253-262, 2000.
39. Panwalkar A, Verstovsek S and Giles FJ: Mammalian target of rapamycin inhibition as therapy for hematologic malignancies. Cancer 101: 1478, 2004.
40. De Young MP, Horak P, Sofer A, Sgroi D and Ellisen LW: Hypoxia regulates TSC1/2-mTOR signaling and tumor suppression through REDD1-mediated 14-3-3 shuttling. Genes Dev 15: 239-251, 2008.
41. McCubrey JA, Steelman LS, Abrams SL, Bertrand FE, Ludwig DE, Bäsecke J, Libra M, Stivala F, Milella M, Tafuri A, Lunghi P, Bonati A and Martelli AM: Targeting survival cascades induced by activation of Ras/Raf/MEK/ERK, PI3K/PTEN/Akt/mTOR and Jak/STAT pathways for effective leukemia therapy. Leukemia 22: 708-722, 2008.

J Pharmacol Sci 108, 535 – 544 (2008)

Journal of Pharmacological Sciences

Full Paper

Inhibition of Peroxisome Proliferator-Activated Receptor γ Promotes Tumorigenesis Through Activation of the β-Catenin / T Cell Factor (TCF) Pathway in the Mouse Intestine

Toshio Fujisawa[1], Michiko Sugiyama[1], Ayako Tomimoto[1], Koichiro Wada[2], Hiroki Endo[1], Hirokazu Takahashi[1], Kyoko Yoneda[1], Masato Yoneda[1], Masahiko Inamori[1], Satoru Saito[1], Yasuo Terauchi[3], Takashi Kadowaki[4], Naoto Tsuchiya[5], Hitoshi Nakagama[5], and Atsushi Nakajima[1,*]

[1]*Division of Gastroenterology,* [3]*Division of Endocrinology and Metabolism, Yokohama City University School of Medicine, 3-9 Fuku-ura, Kanazawa-ku, Yokohama 236-0004, Japan*
[2]*Department of Pharmacology, Graduate School of Dentistry, Osaka University, 1-8 Yamadaoka, Suita, Osaka 565-0871, Japan*
[4]*Department of Metabolic Diseases, Graduate School of Medicine, University of Tokyo, 7-3-1 Hongo, Bunkyo-ku, Tokyo 113-0033, Japan*
[5]*Biochemistry Division, National Cancer Center Research Institute, 1-1 Tsukiji 5-chome, Chuo-ku, Tokyo 104-0045, Japan*

Received July 26, 2008; Accepted October 30, 2008

Abstract. Although peroxisome proliferator-activated receptor γ (PPARγ) is strongly expressed in the intestinal epithelium, the role of PPARγ in intestinal tumorigenesis has not yet been elucidated. To address this issue, we investigated the effect of PPARγ inhibition and its mechanism on intestinal tumorigenesis using a selective antagonist, T0070907. We treated $Apc^{Min/+}$ mice and carcinogen-induced colon cancer model C57BL/6 mice with T0070907 and counted the number of spontaneous polyps and aberrant crypt foci and observed cell proliferation and β-catenin protein in the colon epithelium. To investigate its mechanism, the changes of β-catenin/TCF (T cell factor) transcriptional activity and location of β-catenin induced by T0070907 were investigated in the colon cancer cell lines. T0070907 promoted polyp formation in the small intestine of $Apc^{Min/+}$ mice and aberrant crypt foci in the colon of C57BL/6 mice. PPARγ inhibition promoted cell proliferation and increased expressions of the c-myc and cyclin D1 genes and the β-catenin protein in the colon epithelium. In vitro, cell proliferation was promoted, but it was inhibited by the transfection of dominant-negative Tcf4. T0070907 increased β-catenin/TCF transcriptional activity and β-catenin protein in the cytsol and nucleus, but relatively decreased it on the cell membrane. PPARγ antagonist promotes tumorigenesis in the small intestine and colon through stimulation of epithelial cell proliferation. β-Catenin contributes to the promotion of tumorigenesis by PPARγ antagonist due to activation of TCF/LEF (lymphoid enhancer factor) transcriptional factor.

Keywords: peroxisome proliferator-activated receptor γ (PPARγ), T0070907, aberrant crypt foci (ACF), β-catenin, intestinal tumor

Introduction

Peroxisome proliferator-activated receptor γ (PPARγ), a member of the nuclear receptor superfamily, is involved in the regulation of growth, differentiation, and metabolism of various cell types via transcriptional regulation of target genes (1). PPARγ has been shown to be abundantly expressed in the intestinal epithelium and in colon cancer cells (2). The role of PPARγ in regulating neoplastic transformation, however, remains controversial. Saez and Lefebvre reported that PPARγ ligands promoted colon polyp formation in $Apc^{Min/+}$ mice (3, 4),

*Corresponding author. nakajima-tky@umin.ac.jp
Published online in J-STAGE on December 10, 2008 (in advance)
doi: 10.1254/jphs.08193FP

whereas, in contrast, Sarraf and Tanaka reported that PPARγ ligands inhibited colon carcinogenesis (5, 6). Using $Apc^{Min/+}$ mice, McAlpine showed that PPARγ deficiency enhanced the number of $Apc^{Min/+}$ tumors in both the small intestine and colon (7). In a previous study, we demonstrated the chemopreventive effect of PPARγ ligands against colon cancer development in an azoxymethane (AOM)-induced colon cancer model (8). Niho also demonstrated that PPARγ ligands suppressed tumor formation in $Apc^{Min/+}$ mice (9). These aforementioned findings indicate that activation of PPARγ by its ligands may suppress colon carcinogenesis. However, no studies have investigated the effect of PPARγ inhibition on intestinal tumorigenesis by using a PPARγ-specific antagonist. Therefore, we examined the effects of the PPARγ-specific antagonist T0070907 (10) on colorectal carcinogenesis and its mechanism.

$Apc^{Min/+}$ mice have a mutation of *APC*, which is a major regulator of β-catenin activation, and represent a model of adenomatous polyposis coli (APC) (11). β-Catenin is involved in mediating two major functions in normal cells: a) regulation of cell-cell adhesion as a component of the E-cadherin/catenin adherens complex in the cell membrane and b) mediation of the proliferating signal through the Wingless/Wnt pathway through its expression in the cytoplasm and nucleus (12 – 14). β-Catenin acts as a transcription cofactor with T cell factor/lymphoid enhancer factor (TCF/LEF) in the Wnt signaling pathway. Free pools of β-catenin are tightly regulated by the tumor suppressor proteins, APC and GSK3β, and destabilized by phosphorylation at Ser33, Ser37, and Thr41 (15). Mutations of any of APC or β-catenin itself can lead to inhibition of β-catenin degradation, resulting in an increase in the cytoplasmic pools (16 – 20) and activation of TCF/LEF-mediated transcription.

On the other hand, the relationship between PPARγ and β-catenin was reported in some studies, but it is still unclear for colon cancer. In the maintenance of preadipocytes, activation of β-catenin by overexpression of Wnt or a GSK3β phosphorylation-defective mutant of β-catenin blocks adipogenesis via inhibition of PPARγ-associated gene expressions (21, 22). Conversely, activation of PPARγ by its ligands stimulates the degradation of β-catenin (23). Jansson reported a direct interaction between PPARγ and β-catenin in colon cancer cells (24). From the above, it is evident that β-catenin and PPARγ mutually inhibit each other's activity, and it is thought that a balance between β-catenin and PPARγ signaling is important for the maintenance of normal cell differentiation and proliferation (25).

In this study, we investigated the effect of PPARγ inhibition using a selective antagonist, T0070907, on the development of intestinal polyps in $Apc^{Min/+}$ mice and colonic aberrant crypt foci (ACF) in a carcinogen-induced colon cancer mouse model. Furthermore, we aimed to elucidate the role of β-catenin in the promotion of intestinal tumorigenesis by PPARγ antagonists.

Materials and Methods

Reagents and antibodies

The PPARγ-specific antagonist T0070907 was purchased from Cayman Chemical (Ann Arbor, MI, USA). PPARγ siRNA and polyclonal antibody against PPARγ (H-100) were purchased from Santa Cruz Biotechnology, Inc. (Santa Cruz, CA, USA). Azoxymethane (AOM) and MTT (methylthiazolyldiphenyl-tetrazolium bromide) were purchased from Sigma (St. Louis, MO, USA). Monoclonal antibody against β-catenin and polyclonal antibody against Phospho-β-Catenin (Ser33/37/Thr41) were purchased from BD Transduction Laboratories (San Diego, CA, USA) and Cell Signaling Technology (Danvers, MA, USA), respectively.

Cell lines

The human colon cancer cell lines Lovo and HT-29 were obtained from Health Science Research Resources Bank (Osaka) and American Type Culture Collection (Manassas, VA, USA), respectively.

Animals

The mice were treated humanely according to the National Institutes of Health and AERI-BBRI Animal Care and Use Committee guidelines. All animal experiments were approved by the institutional Animal Care and Use Committee of Yokohama City University School of Medicine. Five-week-old male C57BL/6 mice were purchased from CLEA Japan (Tokyo) and male C57BL/6-*Apc*$^{Min/+}$ mice ($Apc^{Min/+}$ mice) were purchased from the Jackson Laboratory (Bar Harbor, ME, USA). Three to five mice were housed per metallic cage, with sterilized softwood chips as bedding, in a barrier-sustained animal room air-conditioned at 24 ± 2°C and 55% humidity, under a 12-h light/dark cycle.

Spontaneous intestinal polyp formation model

To investigate the effect of PPARγ inhibition on intestinal polyp formation, six-week-old mice were divided into groups of 8 or 9 male $Apc^{Min/+}$ mice per group, and each group was given 0 (control), 25, 50, or 100 ppm of the PPARγ antagonist T0070907, mixed into the diet, for 7 weeks. The daily intake of T0070907 in the 100-ppm group was estimated to be approximately 10 mg/kg body weight based on the diet consumption.

Food and water were provided ad libitum to the animals. The animals were then observed for clinical signs and mortality. The body weights and food consumption were measured weekly. The intestines were divided into three sections: the colon and two segments of the small intestine: proximal (half of oral portion in small intestine) and distal (half of the anal portion in small intestine). These segments were opened longitudinally and fixed in 10% neutral buffered formalin. The number of the polyps was determined by examination under a stereoscopic microscope. Polyps that were bigger than 1.0 mm in the maximum axis were counted.

Induction of ACF in a mouse model of AOM-induced colon cancer

Six-week-old C57BL/6 mice were divided into 2 groups composed of mice treated with 500 ppm T0070907 or not treated. The mice of both groups were given two weekly intraperitoneal injections of 10 mg/kg of AOM. In six weeks after the treatment, the mice were sacrificed and samples were collected. The numbers of ACF and aberrant crypts (ACs) were counted as described previously (8).

Immunohistochemistry of normal colon epithelium

Paraffin-embedded sections were deparaffinized and subjected to immunohistochemical staining for β-catenin with an anti-mouse β-catenin monoclonal antibody using a Vectastain ABC kit (Vector Laboratories, Burlingame, CA, USA) and for BrdU using the staining kits (BD Biosciences, San Jose CA, USA) in accordance with the manufacturer's instructions. The primary β-catenin antibody was diluted 1:800 and nuclear counterstaining was performed with hematoxylin.

BrdU labeling index

The Bromodeoxyuridine (BrdU) labeling index was expressed as the ratio of the number of positively stained nuclei to the total number of nuclei counted in the crypts of the colon. The criteria for selecting the crypts in which to conduct the measurements were as follows: a clearly visualized and continuous cell column on each side of the crypt, a completely visible crypt lumen, and opening of the crypt in the middle area of each colon. Twenty crypts were counted in each mouse, and all animals were evaluated.

Cell proliferation and apoptosis assay

Cell proliferation was measured by the MTT assay. Cells were plated in 96-well plates at a concentration of 5×10^3 cells each well. A 0.4-μg sample of dominant-negative Tcf4 plasmid (26) (kindly provided by Dr. Tetsuji Yamada, Biochemistry Division, National Cancer Center Research Institute) or 0.4 μg of pTRE2-pur as a mock control was transfected using Lipofectamin 2000 (Invitrogen, Carlsbad, CA, USA) in accordance with the procedure recommended by the manufacturer. After the transfection, cells were treated with 10 μM T0070907 for 24 h, and then 0.5% MTT solution was added to each well. The absorbance at 595 nm was determined using a microplate reader (Model 550; Bio-Rad, Richmond, CA, USA). The experiments were performed in quadruplicate and repeated three times.

To evaluate the apoptotic activity, annexin V staining was performed using the Annexin V-FITC Apoptosis Detection kit I (BD Biosciences) in accordance with the manufacturer's instructions. Cells were subsequently analyzed by FACScan flow cytometry.

Inhibition of PPARγ function using siRNA

Lovo cells at 70% confluence were transfected with PPARγ siRNA by Lipofectamin 2000 in accordance with the procedure recommended by the manufacturer. The cells were treated with 10 nM PPARγ siRNA for 24 h. We used Stealth RNAi Negative Control Medium GC (Invitrogen) for the control specimens. Inhibition of PPARγ expression was confirmed by real-time RT-PCR and PPARγ expression was suppressed by over 80% as compared with that in the control (data not shown).

Reporter gene assay

Untreated cells or cells treated with T0070907 or PPARγ siRNA for 24 h were transfected with either 0.4 μg TOPflash (containing TCF/LEF-binding sites, the basic thymidine kinase promoter, and the firefly luciferase reporter gene) (Upstate, Lake Placid, NY, USA) or 0.4 μg FOPflash (containing mutated TCF /LEF-binding sites) (Upstate) by Lipofectamin 2000. All samples were normalized by transfecting 0.1 μg phRL-tk (Promega, Madison, WI, USA). At 24 h after the transfection, luciferase activities were measured with the Dual Luciferase Reporter Assay System (Promega). This experiment was performed in triplicate and repeated three times.

Western blot analysis

Colon epithelial protein was extracted with T-PER (PIERCE, Rockford, IL, USA). Cytsolic and nuclear protein was collected using ProteoExtract Subcellular Proteome Extraction Kit (EMD Biosciences, Darmstadt, Germany). Protein concentrations were determined by using Protein Assay Reagent (Bio-Rad). Protein were separated by SDS/PAGE and transferred to a polyvinylidene difluoride membrane. After the transfer, the membranes were blocked with Blocking One-P (Nacalai Tesque, Kyoto) and probed with each primary antibody.

Horseradish-peroxidase–conjugated secondary antibodies and the ECL detection kit (Amersham, London, UK) were used for the detection of specific proteins. All images were taken by LAS3000 (Fuji Film, Tokyo). The results were normalized to the expression level of GAPDH for the total cell, tubulin for the cytosol, and histone for the nucleus.

Gene expression analysis

Total RNA was extracted from the mouse colon epithelium and colon cancer cell lines, Lovo and HT29, using the RNeasy Mini Kit (QIAGEN). Total RNA was reverse-transcribed into cDNA and amplified by real-time RT-PCR using the ABI PRISM 7700 System (Applied Biosystems, Foster City, CA, USA). The probes and primer pairs specific for cyclin D1, c-myc, PPARγ, and β-actin were purchased from Applied Biosystems. The concentrations of the target genes were determined using the competitive CT method and the values were normalized to an internal control.

Immunofluorescence analysis of colon cancer cells

Colon cancer cells were plated on collagen-1–coated glass coverslips followed by exposure to 10 μM T0070907 for 12 h. The coverslips were paraformaldehyde-fixed and permeabilized with 100% ethanol at −20°C. Fixed cells were incubated with primary antibodies and stained with Alexa Fluoro-conjugated secondary antibodies (Molecular Probes, Eugene, OR, USA). Confocal laser scanning microscopic images were then generated (Carl Zeiss, ObErkochen, Germany). The primary β-catenin antibody and PPARγ antibody were diluted 1:800 and 1:500, respectively.

Statistical analyses

All results are expressed as mean ± S.D. values. Statistical analysis for the multiplicity of the colon tumors was conducted using ANOVA. Other statistical analyses were performed by Student's *t*-test. The results were considered to be statistically significant when P values were <0.05.

Results

Enhancement of spontaneous polyp formation in the $Apc^{Min/+}$ mice by the selective PPARγ antagonist

Fig. 1A shows the number and distribution of intestinal polyps in the $Apc^{Min/+}$ mice treated with the PPARγ antagonist T0070907 or vehicle. Most polyps were observed in the small intestine, with only a few apparent in the colons, both in the T0070907- and vehicle-treated groups. A significant increase in the number of polyps in the distal, but not proximal, portion of the small intestine was observed. Similarly, a significant increase in the total polyp number was observed in the mice treated with the PPARγ antagonist as compared with the control. In contrast, basal spontaneous polyp formation was markedly less pronounced in the colon than in the small intestine in this model. There were no significant differences in the body weights or food intake of the mice among the groups. To examine the effect of T0070907 on adipogenesis, we measured the serum levels of triglyceride, free fatty acid, and total cholesterol in each mouse before it was killed. There was no significant difference among the groups (data not shown). None of the mice died during the observation period.

Inhibition of PPARγ promotes colon epithelial cell proliferation and ACF formation in the mouse model of AOM-induced colon tumorigenesis

Significant increases in the number of ACF and ACs were observed following treatment with the PPARγ antagonist in the colon of the mouse model of AOM-induced tumorigenesis (Fig. 1B).

The expression of PPARγ in the mouse intestine was examined by western blot analysis. PPARγ expression was lowest in the proximal intestine and in the more distal portion showed higher expression (Fig. 1C).

We performed BrdU immunohistochemical staining of the colon epithelium of the mouse model of AOM-induced colon tumorigenesis to investigate the effects of T0070907 treatment on the cell proliferative activity. A significant increase of the BrdU labeling index was observed in the colon of the mice treated with T0070907 as compared with the control mice (Fig. 2A).

Inhibition of PPARγ increases the gene expression level of cyclin D1 and c-myc and protein level of β-catenin in the colon epithelium

Analysis of the gene expressions of c-myc and cyclin D1 in the colon epithelium was performed by real-time RT-PCR. Expressions of both the c-myc and cyclin D1 genes were significantly increased following treatment with T0070907 (500 ppm) (Fig. 2B). Next, we investigated the protein level of β-catenin. Western blot analysis showed β-catenin increased by the treatment of T0070907 (Fig. 2C). These results indicate that the inhibition of PPARγ increases colon epithelial cell proliferation by promoting the transcription of these genes due to β-catenin increase, thereby accelerating the formation of ACF.

Immunohistochemistry of β-catenin in normal colonic epithelium following treatment with T0070907

To investigate changes of quantity and localization

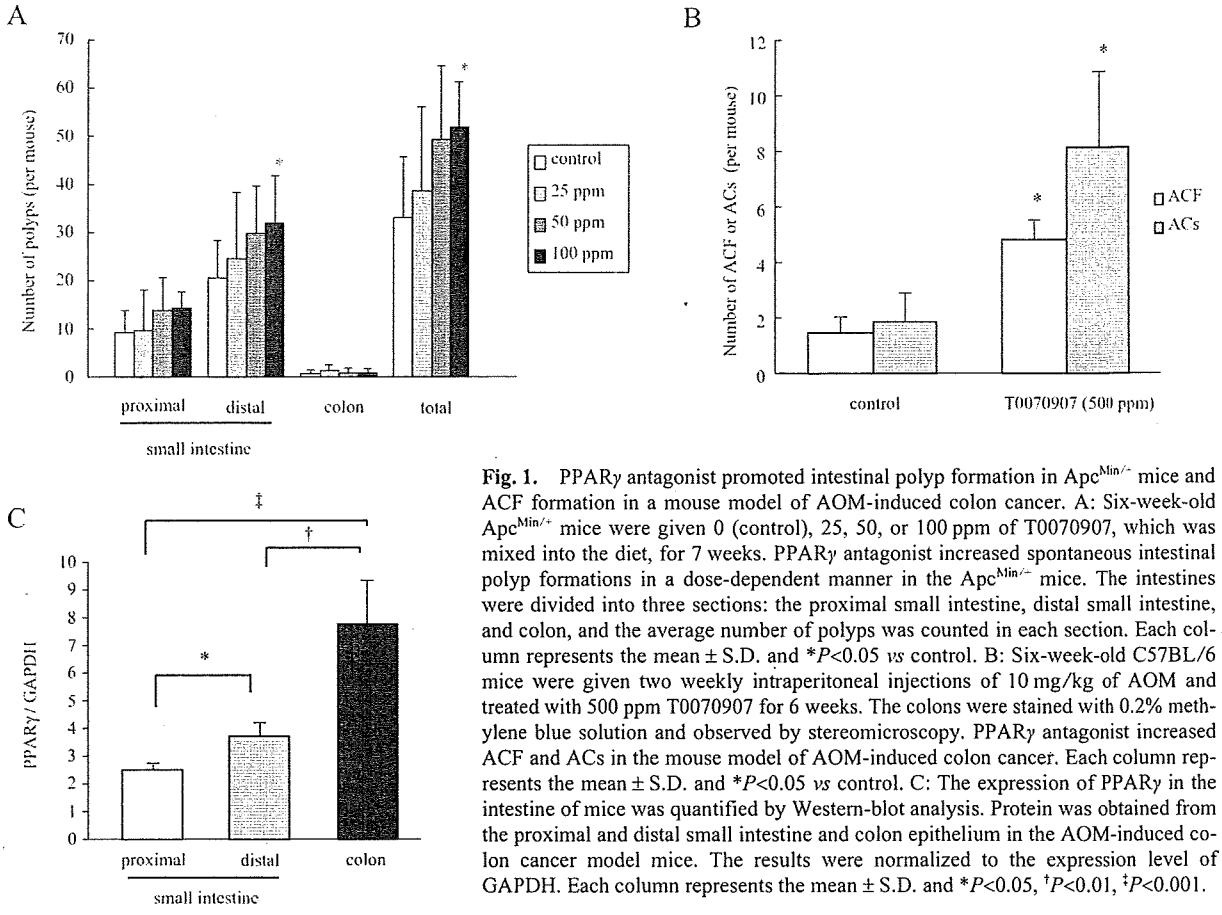

Fig. 1. PPARγ antagonist promoted intestinal polyp formation in $Apc^{Min/+}$ mice and ACF formation in a mouse model of AOM-induced colon cancer. A: Six-week-old $Apc^{Min/+}$ mice were given 0 (control), 25, 50, or 100 ppm of T0070907, which was mixed into the diet, for 7 weeks. PPARγ antagonist increased spontaneous intestinal polyp formations in a dose-dependent manner in the $Apc^{Min/+}$ mice. The intestines were divided into three sections: the proximal small intestine, distal small intestine, and colon, and the average number of polyps was counted in each section. Each column represents the mean ± S.D. and $*P<0.05$ *vs* control. B: Six-week-old C57BL/6 mice were given two weekly intraperitoneal injections of 10 mg/kg of AOM and treated with 500 ppm T0070907 for 6 weeks. The colons were stained with 0.2% methylene blue solution and observed by stereomicroscopy. PPARγ antagonist increased ACF and ACs in the mouse model of AOM-induced colon cancer. Each column represents the mean ± S.D. and $*P<0.05$ *vs* control. C: The expression of PPARγ in the intestine of mice was quantified by Western-blot analysis. Protein was obtained from the proximal and distal small intestine and colon epithelium in the AOM-induced colon cancer model mice. The results were normalized to the expression level of GAPDH. Each column represents the mean ± S.D. and $*P<0.05$, $^{\dagger}P<0.01$, $^{\ddagger}P<0.001$.

of β-catenin in the colon epithelium, we performed immunohistochemistry for β-catenin (Fig. 2D). Imuunohistochemistry revealed no clear difference of the location and the amount of β-catenin between control and T0070907-treated mice.

PPARγ antagonist does not affect the apoptotic activity but increases the cell proliferative activity via TCF/LEF transcriptional factor in colon cancer cells

To elucidate the mechanism underlying the effect of PPARγ inhibition on tumor formation, we investigated the effect of the PPARγ antagonist T0070907 on the cell proliferative and apoptotic activity using the cultured colon cancer cell lines Lovo and HT-29. MTT assay revealed that T0070907 increased the cell proliferative activity of the colon cancer cells (Fig. 3A). Furthermore, knockdown of TCF/LEF transcriptional factor by induction of dominant-negative Tcf4 plasmid inhibited the increase of cell proliferation by T0070907 (Fig. 3: B and C). On the other hand, the assay using annexin V showed no difference in the apoptotic activity between the control and T0070907-treated cells (data not shown).

Inhibition of PPARγ increases the expressions of c-myc and cyclin D1 via transcriptional activation of β-catenin

Real-time RT-PCR revealed that T0070907 significantly increased the gene expressions of both c-myc and cyclinD1 in the colon cancer cell lines Lovo and HT29 (Fig. 4A). We then performed the β-catenin/TCF reporter assay (TOPflash/FOPflash system) to investigate the transcriptional activity of β-catenin. PPARγ antagonist increased β-catenin/TCF reporter activity in Lovo and HT29 cells (Fig. 4B). We checked this effect using PPARγ siRNA, which also increased β-catenin /TCF reporter activity in Lovo cells (Fig. 4C).

PPARγ antagonist increases β-catenin protein by suppressing its degradation

We quantified the protein expression levels of β-catenin in Lovo and HT-29 cells that were left untreated or treated with the PPARγ antagonist. T0070907 increased β-catenin protein level in both cell lines (Fig. 5A). To elucidate the mechanism underlying the increase of β-catenin protein by T0070907, we performed real-time RT-PCR to examine the production of β-catenin and western blot analysis of β-catenin and

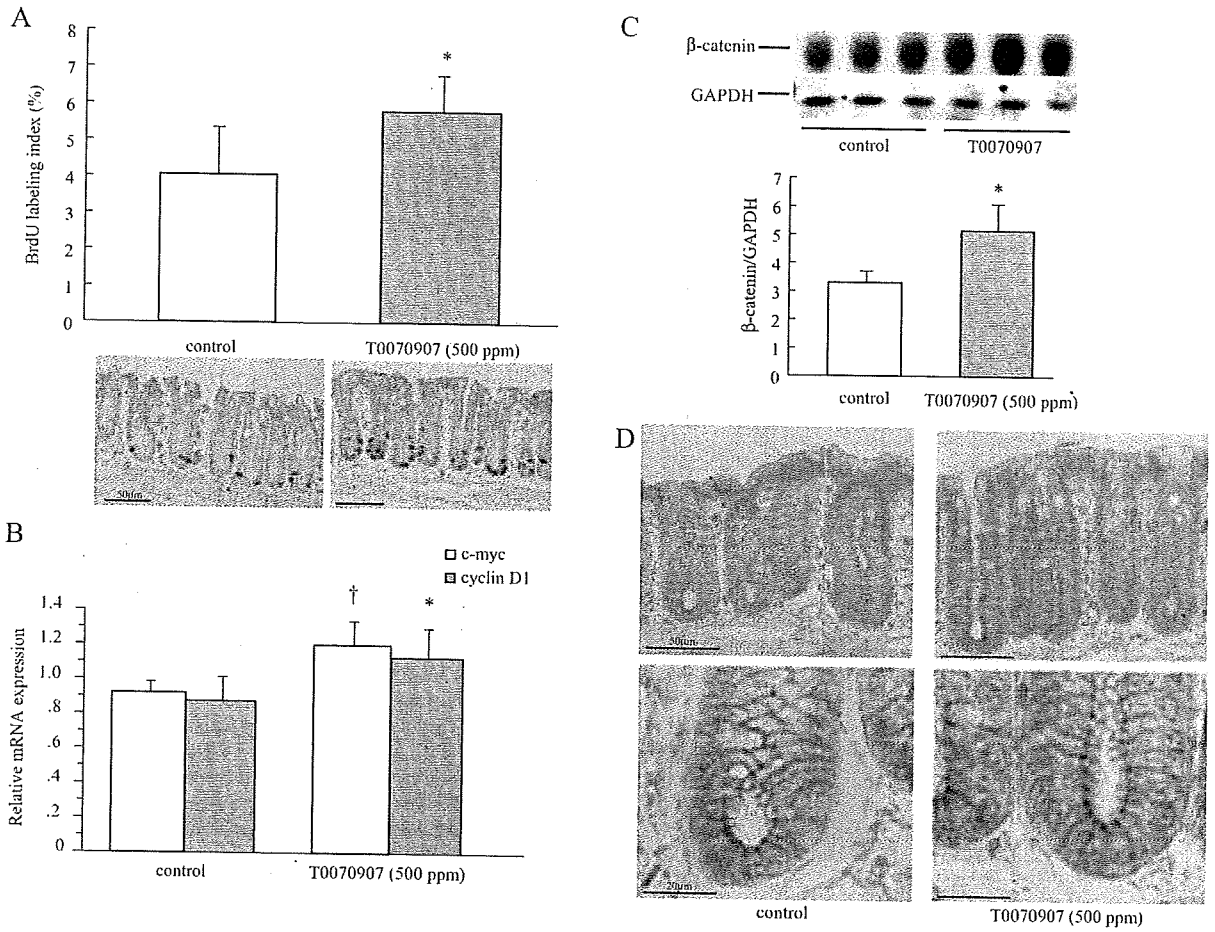

Fig. 2. PPARγ antagonist increased cell proliferation in colon epithelium via increase of β-catenin, c-myc, and cyclin D1 in AOM-induced colon cancer model mouse. A: BrdU was administered intraperitoneally at a dose of 50 mg/kg, 1 h prior to the sacrifice of the mice. BrdU-positive cells were detected by immunohistochemistry. The BrdU labeling index was expressed as the ratio of the number of positively-stained nuclei to the total number of nuclei counted in the crypts of the colon. Lower photographs show representative immunohistochemical staining for BrdU in each group. Each column represents the mean ± S.D. and $^*P<0.05$. B: Real-time RT-PCR analysis for cyclin D1 and c-myc expressions in the colon epithelium. Samples were obtained from normal colon epithelium in the AOM-induced colon cancer model mouse. Each column represents the mean ± S.E.M and $^*P<0.05$, $^\dagger P<0.01$. C: Western blot analysis for β-catenin was performed. Total protein was obtained from normal colon epithelium. Upper photographs showed representative western blot signals for β-catenin and GAPDH. Each column represents the mean ± S.D. and $^*P<0.05$. D: Immunohistochemistry of β-catenin in normal colon epithelium obtained from the AOM-induced colon cancer model mouse. There was no clear difference of the location and the amount of β-catenin between control and T0070907-treated mice. Nuclear counterstaining was performed with hematoxylin.

phospho-β-catenin to examine the degradation of β-catenin. Real-time RT-PCR revealed no difference in the β-catenin mRNA expression level between the control and T0070907-treated cells (data not shown). On the other hand, western-blot analysis revealed an increase in the amount of β-catenin and a decrease in the amount of phospho-β-catenin following treatment with T0070907 (Fig. 5A). These results indicated that T0070907 increased β-catenin protein not due to an increase of β-catenin production, but a decrease of β-catenin degradation.

PPARγ antagonist increases cell proliferation via increase of the β-catenin expression in the nucleus

To confirm the increase of β-catenin expression in the nucleus, we fractionated the cell protein into cytosol and nucleus, and then measured the β-catenin expression in each of the compartments by Western-blot analysis. T0070907 increased β-catenin expression in the cytosol and nucleus (Fig. 5B). Consecutively, we performed immunofluorescent staining for β-catenin and PPARγ to investigate the intracellular localization of β-catenin by confocal microscopy. β-Catenin was strongly expressed on the cell membrane and weakly expressed in the

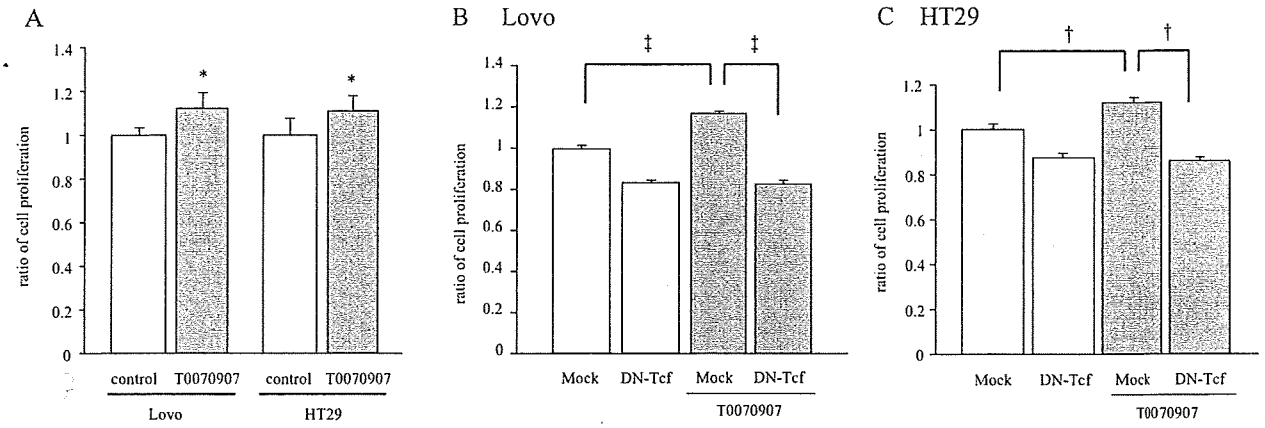

Fig. 3. PPARγ antagonist increased cell proliferation via Tcf4 in the colon cancer cells. A: MTT assay was performed in colon cancer cell lines to examine the effect of PPARγ antagonist for cell proliferation in vitro. Lovo and HT29 cells were treated and untreated with 10 μM T0070907 for 24 h. The PPARγ antagonist significantly increased the cell proliferations in both cell lines. The ratio in the control was defined as 1.0. Each column represents the mean ± S.D. *P<0.05 *vs* control. B and C: Cell proliferation assay in Lovo cells (B) and HT29 cells (C) transfected with dominant–negative Tcf4 (DN-Tcf) or mock vector. At 24 h after transfection, Lovo and HT29 cells were either left untreated or untreated with T0070907 for 24 h. Each column represents the mean ± S.D. $^{\dagger}P$<0.01, $^{\ddagger}P$<0.001 *vs* control.

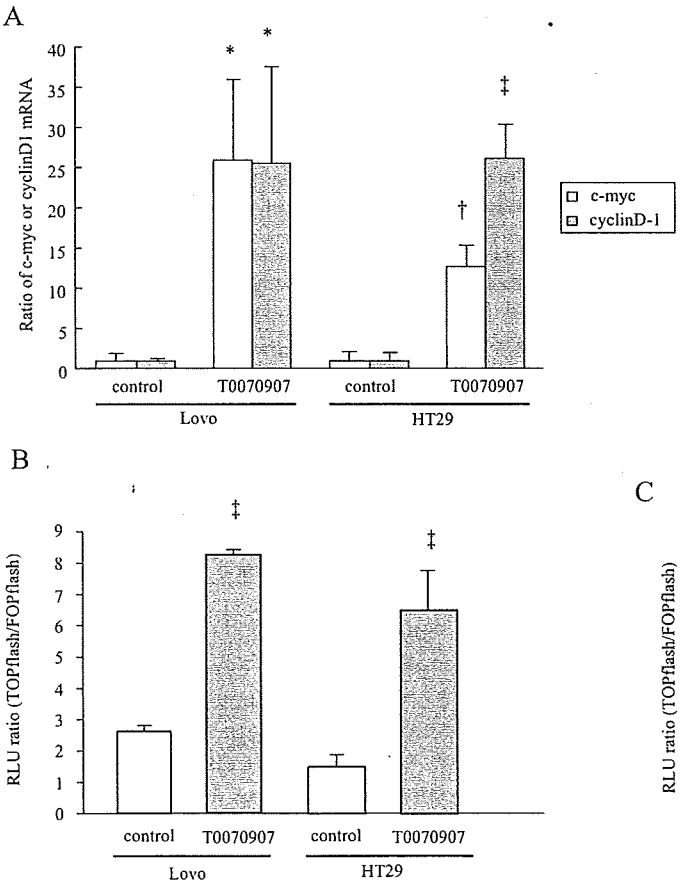

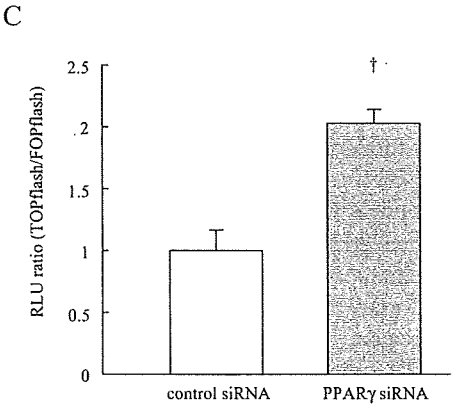

Fig. 4. Inhibition of PPARγ activated β-catenin transcriptional activity and increased c-myc and cyclin D1 in colon cancer cells. A: Real-time RT-PCR for c-myc and cyclin D1 in Lovo and HT-29 cells treated or untreated with T0070907. The values were normalized to the expression level β-actin. Each column represents the mean ± S.D. *P<0.05, $^{\dagger}P$<0.01, $^{\ddagger}P$<0.001 *vs* control. B and C: β-catenin transcriptional activity was examined by transfecting TOPflash and FOPflash in colon cancer cells. After the treatment with 50 μM T0070907, TOPflash or FOPflash was transfected into Lovo cells or HT29 cells (B). At 24 h after treatment with PPARγ siRNA, Lovo cells were transfected with TOPflash or FOPflash (C). The relative light units (ratio of TOPflash to FOPflash) are indicated. Elevation of the β-catenin transcriptional activity was observed following both T0070907- and PPARγ siRNA-induced inhibition of PPARγ. Each column represents the mean ± S.D. $^{\dagger}P$<0.01 and $^{\ddagger}P$<0.001 *vs* control.

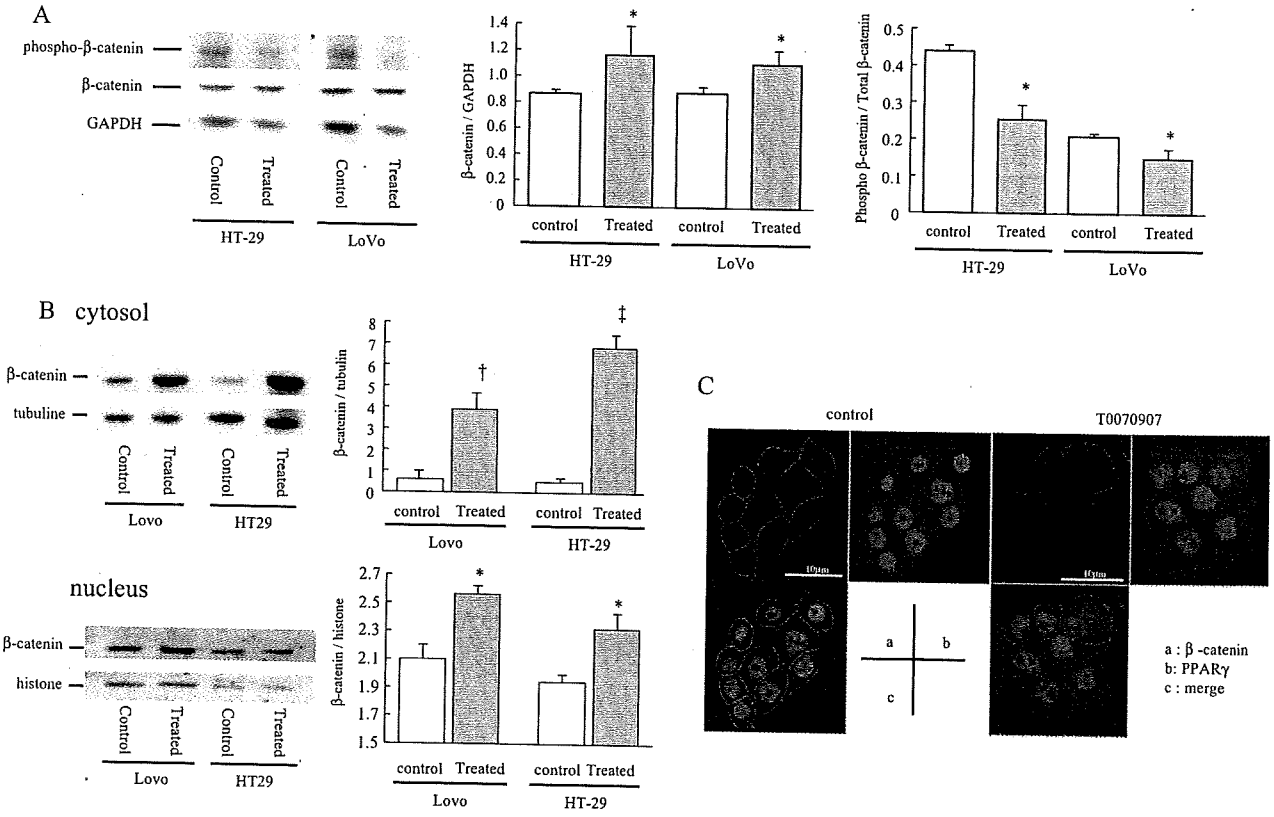

Fig. 5. PPARγ antagonist increased β-catenin protein in the whole cell, cytosol and nucleus by suppressing its phosphorylation. A: Western-blot analysis for β-catenin and phospho-β-catenin (Ser 33/37/Thr 41) was performed in the Lovo cells and HT29 cells. T0070907 increased β-catenin and decreased phospho-β-catenin in the both types of cells. Photographs show representative Western-blot signals for β-catenin, phospho-β-catenin, and GAPDH. Each column represents the mean ± S.D. and $^{*}P<0.05$ *vs* each control. B: Western-blot analysis for β-catenin with the protein extract from the cytosol and nucleus. β-Catenin was particularly increased in the cytosol. Each column represents the mean ± S.D. and $^{*}P<0.05$, $^{\dagger}P<0.01$, $^{\ddagger}P<0.001$ *vs* each control. C: PPARγ (Green) and β-catenin (Red) immunofluorescence in HT-29 cells treated or not treated with T0070907. Treatment with the PPARγ antagonist increased β-catenin protein in the cytosol and relatively decreased it on the cell membrane.

nucleus in the control cells. On the other hand, in the T0070907-treated cells, relative translocation of β-catenin from the membrane to the cytosol was observed (Fig. 5C). PPARγ was localized mainly in the nucleus and did not merge with β-catenin in either the control or T0070907-treated cells.

Discussion

We clearly demonstrated that inhibition of PPARγ using the selective antagonist T0070907 promoted spontaneous polyp formation, even in the absence of any treatment with chemical carcinogens, in the small intestine of $Apc^{Min/+}$ mice. These results strongly indicate that inhibition of the PPARγ pathway alone may be sufficient to accelerate polyp formation in the small intestine of $Apc^{Min/+}$ mice. McAlpine et al. reported that PPARγ deficiency in gene knockout mice enhanced the number of $Apc^{Min/+}$ tumors (7). The present study supports their report. However, the pharmaceutical effect of PPARγ inhibitor on intestinal tumorigenesis was described for the first time in the present study. A significant increase in the number of polyps in the distal, but not proximal, portion of the small intestine was observed. This result may be explained by the higher level of PPARγ expression in the distal portion compared to the proximal portion (Fig. 1C). Moreover, colon polyps in $Apc^{Min/+}$ mice were not increased by treatment with 100 ppm T0070907, but the number of ACF in the AOM-induced colon cancer model mice was increased by 500 ppm T0070907. We speculate two reasons for the discrepancy of these results: 1) Colon carcinogenesis could not be properly evaluated because the number of colon polyps in $Apc^{Min/+}$ mice was very small (less than 1.0 per mouse). 2) The expression of PPARγ in the colon is higher than in the small intestine (Fig. 1C). Therefore, more T0070907 is needed to suppress the effect of PPARγ in the colon than in the

small intestine. However, once the effect of PPARγ was sufficiently inhibited, the difference should be large.

Cell proliferation and β-catenin protein were increased and cyclin D1 and c-myc expressions were up-regulated in the colon epithelium of PPARγ antagonist–treated mice, but the location of β-catenin protein was not changed. These results suggest that inhibition of PPARγ increases colonic epithelial cell proliferation by increasing the β-catenin protein that is promoting transcription of cyclin D1 and c-myc.

To investigate the mechanism, we investigated the effect of PPARγ inhibition on the cell proliferation and apoptotic activity in colon cancer cell lines. PPARγ inhibition increased the cell proliferation but not the apoptotic activity. Cell proliferation increased by the PPARγ antagonist was inhibited by dominant-negative Tcf4 induction. This result supports that the PPARγ antagonist plays its role via TCF/LEF transcriptional factor.

Increase in the β-catenin/TCF transcriptional activity was observed in association with inhibition of PPARγ in cultured cells by reporter assay, with target gene activation, that is, of cyclin D1 and c-myc. As cyclin D1 and c-myc act as factors accelerating the G1/S phase and as proto-oncogenes (27, 28), it appears that PPARγ inhibition promotes cell proliferation and tumorigenesis by accelerating the cell cycle via enhancing β-catenin /TCF transcriptional activation. Similar increase in gene transcriptional activity was also observed following knockdown by PPARγ siRNA.

Because the PPARγ antagonist did not increase the mRNA expression level of β-catenin (data not shown) but decreased the phosphorylation level of β-catenin protein, the compound may increase the amount of β-catenin via suppressing the degradation of β-catenin. Furthermore, in the immunohistchemistry and western blot analysis of colon cancer cells, PPARγ antagonist does not only increase total-β-catenin but also transfers the main location of β-catenin protein from the cell membrane into the cytosol and nucleus. These results may indicate that the PPARγ antagonist stabilizes β-catenin protein mainly in the cytosol and nucleus, and it causes a relative decrease of the β-catenin on the cell membrane.

In conclusion, we clearly demonstrated that inhibition of PPARγ using a selective antagonist promoted both spontaneous polyp formation in the small intestine of $Apc^{Min/+}$ mice and carcinogen-induced ACF formation in the colon. Inhibition of PPARγ increased β-catenin expression especially in the nucleus, resulting in enhanced expression of cyclin D1 and c-myc via TCF /LEF transcriptional factor, which in turn, promoted epithelial cell proliferation. Our results imply that PPARγ plays an important role of suppressing tumorigenesis in the intestine by attenuating epithelial cell proliferative activity.

Acknowledgments

We thank Machiko Hiraga for her technical assistance. This work was supported in part by a Grant-in-Aid for research on the Third Term Comprehensive Control Research for Cancer from the Ministry of Health, Labour, and Welfare, Japan to A.N.; a grant from the National Institute of Biomedical Innovation to A.N.; and a grant from the Ministry of Education, Culture, Sports, Science, and Technology, Japan, (KIBAN-B) to A.N.; a grant from the Princess Takamatsu Cancer Research Foundation to A.N.; and a grant from the Japanese Human Science Research Foundation to A.N.

References

1 Debril MB, Renaud JP, Fajas L, Auwerx J. The pleiotropic functions of peroxisome proliferator-activated receptor gamma. J Mol Med. 2001;79:30–47.
2 DuBois RN, Gupta R, Brockman J, Reddy BS, Krakow SL, Lazar MA. The nuclear eicosanoid receptor, PPARgamma, is aberrantly expressed in colonic cancers. Carcinogenesis. 1998; 19:49–53.
3 Saez E, Tontonoz P, Nelson MC, Alvarez JG, Ming UT, Baird SM, et al. Activators of the nuclear receptor PPARgamma enhance colon polyp formation. Nat Med. 1998;4:1058–1061.
4 Lefebvre AM, Chen I, Desreumaux P, Najib J, Fruchart JC, Geboes K, et al. Activation of the peroxisome proliferator-activated receptor gamma promotes the development of colon tumors in C57BL/6J-APCMin/+ mice. Nat Med. 1998;4:1053–1057.
5 Sarraf P, Mueller E, Jones D, King FJ, DeAngelo DJ, Partridge JB, et al. Differentiation and reversal of malignant changes in colon cancer through PPARgamma. Nat Med. 1998;4:1046–1052.
6 Tanaka T, Kohno H, Yoshitani S, Takashima S, Okumura A, Murakami A, et al. Ligands for peroxisome proliferator-activated receptors alpha and gamma inhibit chemically induced colitis and formation of aberrant crypt foci in rats. Cancer Res. 2001;61:2424–2428.
7 McAlpine CA, Barak Y, Matise I, Cormier RT. Intestinal-specific PPARgamma deficiency enhances tumorigenesis in ApcMin/+ mice. Int J Cancer. 2006;119:2339–2346.
8 Osawa E, Nakajima A, Wada K, Ishimine S, Fujisawa N, Kawamori T, et al. Peroxisome proliferator-activated receptor gamma ligands suppress colon carcinogenesis induced by azoxymethane in mice. Gastroenterology. 2003;124:361–367.
9 Niho N, Takahashi M, Kitamura T, Shoji Y, Itoh M, Noda T, et al. Concomitant suppression of hyperlipidemia and intestinal polyp formation in Apc-deficient mice by peroxisome proliferator-activated receptor ligands. Cancer Res. 2003;63: 6090–6095.
10 Lee G, Elwood F, McNally J, Weiszmann J, Lindstrom M,